HIGH PRECISION SPATIAL AND TEMPORAL CONTROL OF NEURAL CIRCUITRY USING SEMI-AUTOMATED, MULTI-WAVELENGTH NANOPATTERNING SYSTEM

by

NAGASANDHYA MITNALA

Presented to the Faculty of the Graduate School of
The University of Texas at Arlington in Partial Fulfillment
of the Requirements
for the Degree of

MASTER OF SCIENCE IN BIOMEDICAL ENGINEERING

THE UNIVERSITY OF TEXAS AT ARLINGTON
AUGUST 2009

I dedicate this thesis to ‘thatha’ and ‘Sadasivudu Sir’ who have always been an inspiration of my life

ACKNOWLEDGEMENTS

I wish to take this opportunity to express my gratitude to all individuals who have helped me during this thesis work. I would like to thank my supervising professor Dr. Harold 'Skip' Garner, for being an extremely inspiring and encouraging mentor and providing me with invaluable advice in the course of my graduate degree. Special thanks and appreciation to Dr. Michael Huebschman for his very valuable suggestions and insights into this project, for being a great friend and who would be the first person I would approach regarding my findings in the thesis work.

I am extremely grateful to Dr. George Alexandrakis and Dr. Jian Yang for their interest in my research work and for accepting the invitation to be my committee members. I also express my sincere gratitude to Ms. Amruta Joshi who made me comfortable adapting to lab culture and who was my very first mentor in the lab; to Dipen, who has more than once helped me in dealing with the technical issues in my project; to Linda and Kay for all the administrative help and friendly encouragement they have showered me with, and to all the Garner lab members. I wish to express my gratitude to John and Zack for helping me with the plasmids and the cells. I wish to thank Christian and the entire Herz lab for initially supporting me with the cells. I also wish to thank my friends, who have helped me in every possible way in order for me to complete this thesis. I would like to thank 'Saila pinni' and 'Suresh Babai' for their never ending support.

And most importantly, I am deeply indebted to my family, my parents 'Mommy' and 'Nanna', and my little brother Santosh, who have always been there for me. I would not have made it this far without their help, encouragement and support throughout my life. I love them and am grateful to them more than words can ever express. Special thanks to Leela Aunty, Ajay Uncle and Ginny who let me stay with them during the last six months of my thesis work and

gave me all the love and support that I always received from my family. Above all, THANK YOU GOD for making my life so special with so many special people in it. It is ultimately the faith in YOU that taught me patience and perseverance.

May 13, 2009

ABSTRACT

HIGH PRECISION SPATIAL AND TEMPORAL CONTROL OF NEURAL CIRCUITRY

USING SEMI-AUTOMATED, MULTI-WAVELENGTH

NANOPATTERNING

SYSTEM

NagaSandhya Mitnala, MS

The University of Texas at Arlington, 2009

Supervising Professor: Harold 'Skip' Garner

The ideal way to manipulate neurons would be to reversibly activate and inactivate neuronal firing and thus enable a bi-directional control. Many attempts have been made in the past to have such a tool. The traditional approach for controlling neural circuits is to generate a local electric field which has been shown to be highly effective at triggering action potentials in neurons [53]. Although the timing of the electrode stimulation is very precise, its specificity and spatial control are poor. Also, silencing neuronal activity is as important as stimulating it. Ed Boyden described a protein that switches off nerve firing when activated by light. Karl Deissoroth described the fuller story of the protein called NpHR (Natronomonas pharaonis)[62]. This allows for a spatially and temporally precise neural silencing. Earlier, Boyden worked on a channel for positively charged ions (such as calcium) that is found in green algae and is activated by blue light. This channel, ChR2 was transplanted into mammalian neurons and it was possible for the first time to stimulate a nerve remotely at speeds closer to normal neuronal transmission [52]. The newly discovered NpHR protein is a chloride pump which silences physiological activity, when activated by yellow light. NpHR, in spite of it being a pump rather than a channel, operates at a speed close to that of ChR2 leading to a close to perfect temporal

precision. Using these two proteins to alternately switch the neurons on and off, a bi-directional optical control switch could be obtained. In Zhang, et al's work published in April 2007, groups of neurons (cholinergic motor neurons) were targeted to control bi-directional locomotion. This opened a new gateway for a multimode, high-speed, genetically targeted, all-optical interrogation of living neural circuits [50].

However, there is a need for spatial precision along with temporal precision. This need, leading to a method for precise spatial control of neuronal circuitry along with temporal controls will be discussed in this thesis. With spatial resolution, one could go a step further and interrogate inter neuronal connectivity instead of targeting clusters of neurons.

The aim of the work presented here was to target individual neurons and their inter-connectivity. For this purpose, a novel instrument was built which is an inter-disciplinary project that includes cutting edge technologies such as the DLP (Digital Light Processing) technology, genetically engineering the embryonic neurons to express two protein channels (NpHR and ChR2); and isolation and culture of these neurons. This work also used standard laboratory techniques such as the fluorescence microscopy and optics.

TABLE OF CONTENTS

LIST OF ILLUSTRATIONS

LIST OF TABLES

CHAPTER 1

INTRODUCTION AND BACKGROUND

It is one of the most discussed topics in eons of time- the quest to control the human brain has been the most intriguing research topics for many years now. To precisely control neural circuitry, to understand the neural activity patterns and how they mediate computation, behavior and pathology has been a dream yet to be achieved for the human beings. Researchers, Neurologists and Psychiatrists have equally strived for a simple tool to control the complex web of neural circuits. The outcome of which is the availability of a myriad tools tested and in use for advancing research in the field of neurology.

Neurons respond to electrical signals on a millisecond time scale (or faster) unlike other cells in the body. Electrode stimulation is the most commonly used laboratory technique in the study of excitable cells as of today. However, there are some limitations that have to be overcome and new techniques invented to further neurological studies. The following sections discuss this topic.

1.1 Need for New Techniques to Investigate Brain Development, Organization, and Function

There has been an incredible amount of progress in the understanding of the development, organization, and function of the brain by combining diverse technologies like electrophysiology, anatomy, biochemistry, genetics, psychophysics, neurology, and computational theories. Nevertheless, how this intricate network is built during development and how the brain performs its marvelous functions remains a mystery. This can be attributed to the gap between the brain's enormous complexity and the limited capabilities of the current research tools and conceptual frameworks.

The most fundamental questions remain unanswered in the nervous system beginning with the physiological functioning of single neurons with respect to other neurons and ending at

the physiological functioning of the intact brain. The active and passive functional properties of neurons are not yet known, though their structural properties are well documented. Therefore, it is not fully understood as to how the basic computational elements work and their contribution to the functioning of the very complicated intact neural network as a whole. The neuronal networks resulting from these interconnections have complex properties of their own, in addition to the intrinsic electrical properties of individual constituent neurons [1]. The cellular basis of modification of network function by activity of the network (learning) or the ways information is stored and retrieved by a neuronal network is beginning to be understood only at the level of single neurons in invertebrates, not at the network level. In the vertebrate brain, there is a large redundancy in neuronal networks, and a particular function is probably controlled by the overall activity of large neuronal assemblies rather than by activity of single neurons. The organization and interactions between neuronal assemblies are not understood in the intact brain or even in simplified brain slice preparations. Although a lot has been learned from the now classic anatomic and physiological approaches, there is clearly a need for research tools better equipped to investigate the detailed properties of individual neurons on the one hand and the interactions between large numbers of neurons on the other hand.

1.2 Potential of Optical Imaging Relative to Current Techniques

Optical monitoring of neuronal activity is one of the approaches that offer great promise in giving new information. However, in most cases this approach has been difficult to use and has many limitations. Much effort was thus invested in developing this technique which requires interactions between neurobiology, organic chemistry, spectroscopy, optics, electronics, electro-optics, and computer hardware and software. The rational for investing this effort was the conviction that optical imaging, could substantially add to the information derived by alternative methodologies.

In the past, the use of microelectrodes, mostly to study single neurons, was the only approach with both the spatial and temporal resolution required to investigate the real-time function of individual neurons or neuronal networks. However, microelectrode recordings have two major limitations. First, intracellular microelectrode recordings usually cannot provide simultaneous recordings from more than one site on the neuron's arborization, thus severely hampering the investigation of the microcircuitry [1]. Second, the study of neural networks requires simultaneous recording from many individual neurons. However, the microelectrode recordings are usually limited to two or three neurons. An example can be mentioned in this context. "Understanding of the functional organization of the mammalian cortex is a prerequisite for investigations of cortical information processing or higher brain functions. A complete picture of the functional architecture of even a well-studied cortical area is difficult to achieve with multiple microelectrode penetrations." [1]. Clearly, there is a need for techniques of monitoring patterns of evoked cortical activity with high spatial and temporal resolution. Other approaches lack some of the advantages of electrophysiology techniques. This includes 2-deoxy-D-glucose method (2-DG) [2]. 2-DG permits postmortem visualization of active brain areas or even of single neurons [3, 4], but the time resolution is minutes or hours rather than milliseconds.

In contrast to electrophysiology, optical imaging techniques offer potential advantages: 1) simultaneous recordings of many points in the dendritic or axonal arborization of single neurons; 2) simultaneous recordings from many single neurons; 3) recording of the summed intracellular activity of neuronal populations, including dendrites, axons, or nerve terminals; 4)imaging of spatiotemporal patterns of activity of neuronal populations with millisecond time resolution in vitro and in vivo; and 5) the possibility of repeating measurements from the same area with different experimental conditions or stimulation parameters over an extended time.

The first optical recording of neural activity was made by Hill and Keynes [5], who detected light-scattering changes in active nerves. In general, it is advantageous to use intrinsic optical signals rather than optical signals derived from extrinsic optical probes since the extrinsic

optical probes might modify the investigated system in which they are incorporated. The first optical detection of neuronal activity from a preparation stained with an extrinsic voltage-sensitive dye was reported by Tasaki and collaborators [6] in 1968 and then by Patrick and colleagues [7] in 1971. The demonstrations that optical imaging can provide useful information not easily obtainable by alternative methodologies from a large variety of preparations including single neurons maintained in culture [8,9,10,11,12], invertebrate ganglia [1,13,14,15], brain slices and semi-intact preparations [16,17], and the intact vertebrate brain [18,19,12,20,21) made optical recording a practical and attractive tool.

Newer optical techniques include Positron Emission Tomography (PET) and fMRI (functional Magnetic Resonance Imaging). PET [22] offers three-dimensional localization of active regions in living brain but has both low temporal and low spatial resolution. However, newer PET techniques could be used to study single cell recordings [23]. This technology uses radioactive isotope of oxygen. Since oxygen uptake is related to brain activity, this allows for the spatial mapping of various activities in different parts of the brain during a task. It has a good spatial resolution but relatively bad temporal resolution as an image acquisition can take about 20 seconds.

Neurons, like any other cell in the body, require oxygen to function normally. This oxygen is supplied through the blood flow. The blood supply to the brain is dynamically regulated such that active neural circuits receive more energy and inactive networks receive less energy [24]. fMRI (functional Magnetic Resonance Imaging) is a specialized MRI (Magnetic Resonance Imaging) scan which measures the haemodynamic response related to neural activity in the brain or spinal cord of humans or other animals. The spatial resolution of this type of scan is moderate. Images can be acquired at the rate of 1-4 seconds and the voxels (volumetric pixel) in the acquired images represent about 2-4 millimeters on each side in humans [25].

With every technique invented, the need for improving the spatial resolution becomes increasingly necessary. The above mentioned techniques were nowhere close to the spatial resolution provided by microcopy. Hence, researchers tried to improve this piece of science to look into the cellular and sub-cellular features that were never before imaged. As an effort towards completely eliminating the usage of electrophysiology, optical techniques were employed to measure the readout; whereas in traditional electrophysiology, both the input and output are applied and measured respectively using electrodes. The usage of various dyes for readout is detailed below. Also, the subject has been dealt with by discussing some of the first techniques in optical recordings.

1.3 Principle of Optical Imaging of Neuronal Activity with Dyes

Optical imaging can be accomplished by tagging different structures in the neurons with different dyes. The dyes that have been identified for readout are discussed in this section.

1.3.1 Voltage sensitive dyes

In this technique, voltage sensitive probe molecules are used to vitally stain a preparation [26]. The bath-applied dye molecules bind to the external surface of excitable membranes and act as molecular transducers that transform changes in membrane potential into optical signals. The resulting changes in the absorption, the birefringence, or the emitted fluorescence of the stained neurons linearly correlate with their electrical activity; these changes are monitored with light-measuring devices. The dye response time is usually in the microsecond range [26, 27, 28, 29, 30]. An optical recording of an action potential and a simultaneous electrical recording is demonstrated in the paper titled “Optical Imaging of neuronal activity” [1]. The paper determines that the time course of the two is nearly identical. Also, with the use of an array of photodetectors positioned in the microscope image plane, the activity of many individual targets could be detected simultaneously.

1.3.2 Calcium imaging using fluorescent dyes

Calcium indicators can generally be classified into two types [31]: Chemical indicators and genetically encoded indicators (GECI). Chemical indicators are small molecules that can chelate calcium ions. These molecules are based on an EGTA (ethylene glycol tetraacetic acid- a chelating agent) homologue called BAPTA (1, 2-bis (o-aminophenoxy) ethane-N, N, N', N'-tetraacetic acid) with high selectivity for calcium (Ca2+) ions versus magnesium (Mg2+) ions. This group of indicators includes fura-2, indo-1, fluo-3, Calcium Green-1 (includes both ratiometric and non-ratiometric dyes). These dyes are generally used with the chelator carboxyl groups marked as acetoxymethyl esters in order to render the molecule lipophilic and to allow easy entrance into the cell. Once the indicator is in the cell, cellular esterases will free the carboxyl and the indicator will be able to bind calcium.

GECIs are fluorescent proteins derived from green fluorescent protein (GFP) or its variants (e.g. circularly permuted GFP,YFP,CFP), fused with calmodulin (CaM) and the M13 domain of the myosin light chain kinase, which is able to bind CaM. These indicators do not need to be loaded onto cells, instead the genes encoding for these proteins can be easily transfected to cell lines. It is also possible to create transgenic animals expressing the dye in all cells or selectively in certain cellular subtypes. Regardless of the type of indicator used, the imaging procedures are very similar. Spectral properties of the dye change upon binding to calcium. For example, the indicators might fluoresce only after binding to calcium or the excitation and emission characteristics might change upon binding to calcium. A specific example would be in the case of fluo-3 dye wherein the emission characteristics of the dye change upon binding to calcium. This change in fluorescent intensity could be captured by a CCD camera and analyzed to reflect upon the calcium status. Although a variety of calcium indicators are available and in use, a summary of ratiometric and non-ratiometric dyes are briefed in Tables 1.1 and 1.2 [32].

Table 1.1 Summarizes some of the Ratiometric Calcium indicators that can be used for calcium activity readout. The Table summarizes some of the Ratiometric Calcium indicators, their spectral characteristics, their dissociation constants (K_d), forward ($K_{[+1]}$) and reverse rate constants ($K_{[-1]}$)

Indicator	Absorption maxima (nm)		Emission maxima (nm)		K_d(μM)	K_d(mM)	$K_{[+1]}$ (10^7 M^{-1} s^{-1})	$K_{[-1]}$ (s^{-1})
	Ca^{2+}-bound	Ca^{2+}-free	Ca^{2+}-bound	Ca^{2+}-free	Ca^{2+}	Mg^{2+}	Ca^{2+}	Ca^{2+}
Benzothiaza 1	325	368	468	511	0.66	NA	NA	NA
Benzothiaza 2	325	368	469	479	1.4	NA	NA	NA
Fura-2	335	363	505	512	0.15-0.25	NA	40	103
Indo-1	331	349	410	485	0.25	NA	NA	NA
BisFura-2	338	366	504	511	0.37-0.47	NA	55	257
Fura Red	472	436	645	640	0.13	NA	NA	NA
BTC	401	464	529	533	7-26	NA	0.5	1000

Table 1.2 Summarizes some of the Nonratiometric Calcium indicators that can be used for calcium activity readout. It summarizes some of the Nonratiometric Calcium indicators, their spectral characteristics, their dissociation constants (K_d), forward $K_{[+1]}$ and reverse rate constants $K_{[-1]}$.

Indicators	Absorption maxima (nm)		Emission maxima (nm)		K_d(μM)	K_d(mM)	$K_{[+1]}$ (10^7 M^{-1} s^{-1})	$K_{[-1]}$ (s^{-1})
	Ca^{2+}-bound	Ca^{2+}-free	Ca^{2+}-bound	Ca^{2+}-free	Ca^{2+}	Mg^{2+}	Ca^{2+}	Ca^{2+}
Fluo-3	503	506	526	526	0.39-0.52	8.1	71	369
Fluo-4	494	491	516	516	0.35	NA	NA	NA
Calcium Green-1	506	506	534	533	0.16-0.19	NA	75	120
Calcium Green-2	506	506	531	531	0.53-1.8	NA	NA	NA
Calcium Orange	554	555	575	576	0.33-4.61	NA	NA	NA
Calcium Crimson	588	588	611	611	0.21-0.4	NA	NA	NA
Oregon-Green 488 BAPTA-1	494	494	523	523	0.17	NA	NA	NA
Oregon Green 488 BAPTA-2	494	494	523	523	0.38-0.58	NA	NA	NA
Rhod-2	552	549	581	581	0.57-2.3	NA	NA	NA

1.3.2.1 Quantitative readout of calcium

The best way to measure the readout would be to measure the intracellular calcium levels as a quantitative replication of the activity of the channels. Among the various types of Ca^{2+} indicators, the fluorescent probe Fura-2/AM and Fluo-3 AM are used in this work. It combines high sensitivity and easy diffusion into cells as an uncharged ester. This avoids the local trauma of microinjection through mechanically fragile membranes. The ratio of fluorescence signals excited at two different wavelengths (usually 340/380nm) is found. From this ratio, using Grykiewicz equation [34], the actual concentration of intracellular calcium could be found. Also, it was found in a study conducted by Gailly [33] that this ratio does not depend on probe concentration, cell thickness and setup sensitivity (ex. loading of fura-2 in the cells).
With the development of optical techniques for readout, several different studies, described below, were carried out on neurons.

1.4 Studies of Neuronal Populations in Vertebrate Preparations in Vitro

1.4.1 Visualization of spatiotemporal patterns of population activity in slices

The development of brain slice preparation [35, 36, 37, 38] provided neurobiologists with a method to investigate many questions that could not be investigated in the intact brain in vivo. The hippocampal slice preparation is particularly “convenient” for optical imaging of neuronal populations. This is because of the high degree of stratification among its various neuronal elements, readily observed in transverse brain slices. A given photodetector will receive signals from several presynaptic and/or postsynaptic neuronal elements when stained by a bath application of the dye. Thus optical recordings provide monitoring of “intracellular population activity”, which is the weighted sum of the intracellular membrane potential changes from all of the cellular elements under a given photodetector [1]. The contribution of each cellular element depends on its area, the density of bound dye, its sensitivity at that site, as well as the change in membrane potential. In the transverse hippocampal slice, the high degree of segregated spatial organization of various cellular elements permits intracellular population

recordings from relatively well-resolved populations of neuronal elements, i.e., dendrites, cell bodies, and axons.

1.4.2 Optical recording from isolated and intact brain structures

In vitro studies of semi-intact but isolated brain structures offer an advantage relative to brain slice preparations. The input, output, and other long range synaptic connections are left intact in this technique. Also, the signals are larger than in slices, because a large fraction of neurons and of synaptic connections is left intact. One of the main advantages of optical recording is the imaging of spatiotemporal patterns of electrical activity as described below.

1.4.2.1 Visualization of connectivity between neuronal populations in living brain

Extracellular injection of horseradish peroxide [39] in a given cortical site facilitated postmortem visualization of connectivity in neural network that have projections in the injected site. Orbach and Van Essen [40] have demonstrated that such measurements could provide a powerful tool for pathway tracing. In addition to tracing connections, such experiments may also provide information about the functional properties of the connection involved. Also, they can be combined with local injections of specific drugs to study the nature of synaptic transmission at the site of interest.

1.5 Imaging single cell and subcellular components of neurons

Conventional optical microscopes are used in imaging biological specimens because of their cheap availability, non-invasiveness, flexibility of operation in liquid or air and the possibility of spectroscopic labeling. However, their resolution is diffraction limited to the order of the wavelength. To surpass this diffraction limit, many attempts are being made.

Neurons are largely studied by electron microscope and other varieties of optical microscope such as differential interference contrast microscope (DIC) and confocal microscope. However, with electron microscopes, there are several disadvantages such as the surface information is lost due to use of special sample preparation techniques such as ultra thin sectioning employed in the case of transmission electron microscope and surface coating

used in the case of scanning electron microscope (SEM). The observations are destructive and require high vacuum. With DIC and confocal microscopes, surface information could be retained. However, resolution is limited to the order of the wavelength. The following sections describe the techniques that were proven to be effective in imaging neurons and their sub-cellular structures beyond the diffraction limit of light microscopes.

1.5.1 Observation of nanostructures in neurons using PSTM

In photon scanning tunneling microscope (PSTM), the sample is illuminated under total internal reflection and the localized three dimensional evanescent field generated over the sample is scattered by a sharpened probe tip that has a radius of curvature at its top [41]. According to Maheswari et al, the volume of localization of the evanescent field is proportional to the spatial features (size and shape) of the sample and hence it is possible to detect features of higher spatial frequencies present in the sample with the sharpened probe tip. This process can be considered as the tunneling of evanescent photons from the sample to probe and it obeys the principle of reciprocity in the sense that the process is the same even when the positions of the sample and the probe are interchanged. In other words, the sample scatters the evanescent field generated by the sharpened probe tip. The sample to probe tunneling was referred to as 'collection mode PSTM' and the probe to sample tunneling was referred to as 'illumination mode PSTM'. In the study conducted by Maheswari et al. [41], subcellular structures of neurons were observed with PSTM operated in illumination mode since neurons are thick and difficult to be imaged in collection mode. This is due to the larger absorbance of the thick neurons leading to very weak signals in collection mode.

The PSTM by illumination mode however was useful in imaging microtubules present inside the neural processes of neurons. It was shown by Maheswari et al that PSTM excludes the necessity of removing the cell membrane to observe microtubules using AFM and electron microscope. The full width half maximum of the narrowest tube was found to be 26nm using PSTM. However, the size of the microtubule was found to be 25nm using an electron

microscope. Hence it was found that the resolution of PSTM was almost as high as that of electron microscope.

1.5.2 Two-photon microscopy for reduced photodamage

Light microscopy is used to a large extent because of its high spatial resolution. As observed earlier, techniques like MRI can neither resolve subcellular structures nor provide the exquisite molecular selectivity that allows the detection of single molecules from a background of billions of other molecules. A major innovation towards overcoming the disadvantages of three-dimensional light microscopy was confocal microscopy. However, the wasteful excitation as a result of absorption in the entire specimen but imaging only in a particular focal plane has caused the researchers to opt for multi photon microscopy. Thus two-photon microscopy was adopted. This type of imaging allows for only those molecules that are targeted to be excited thus avoiding photodamage to those areas that are not targeted. Three dimensional imaging of brain slices using multi-photon laser scanning microscope (for two-photon imaging technique) was carried out [42] and the spatial resolution of neurons that could be achieved both invitro and invivo was inspiring.

1.6 Optical Stimulation of Neurons

1.6.1 Infrared Nerve Stimulation

There have been many attempts at stimulating the neural activity using a variety of lasers. Recently, researchers at Vanderbilt University (Nashville, Tennessee) spurred a new field when they successfully stimulated the rat sciatic nerve using pulses of infrared light. Their initial studies documented the advantages of infrared nerve stimulation (INS) over standard electrical stimulation methods: improved spatial selectivity, lack of a stimulation artifact in the recorded response, and non-contact stimulus delivery (infrared nerve stimulation: hearing by light). After successfully stimulating the peripheral motor and sensory nerves with IR wavelength laser light, researchers are now trying to stimulate regions of the Central Nervous system mainly because of the high spatial selectivity of the optical technique employed by them. Action

potentials locked in time with the laser pulses were observed at locations of neural projections several millimeters away from the site of stimulation [43].According to the researchers, when compared to electrically stimulated responses, the optical signal included a smaller volume of stimulated neurons and lack of noise artifact in the recording.

1.6.2 Manipulating neurons to respond to light

Photostimulation eventually started replacing electrode stimulation. There are variations in these techniques: light mediated 'uncaging' of chemically modified signaling molecules, chemical modification of ion channels and receptors to render them light responsive and introduction of light-sensitive proteins into otherwise light-insensitive cells [44].

"Channelrhodopsin-2 and optical control of excitable cells" [44] gives a detailed table on the optical methods to trigger neurons. The table shows temporal, spatial and technical properties of different photostimulation techniques [44]. From the table, it is clear that glutamate uncaging and ChR2 achieve responses on a millisecond time scale, thus imitating the physiological neuronal transmission.

Neurons possess ion channels that are gated by voltage, ligands and temperature but not by light. Thus they have to be structured or engineered to be able to respond to light. Naturally occurring photoreceptive proteins such as rhodopsin, have a covalently attached chromophore that activates the protein on exposure to light. Light can be used to (1) indirectly activate receptor proteins by making a ligand available from a caged precursor or (2) light could be used to directly photoisomerize a synthetic molecule that is covalently attached to a protein and hence imposing conformational changes. Mathew Banghart et al [45] have combined both these ideas by synthesizing a photoisomerizable tether that attaches a specific ligand on a protein near its normal binding site. This allows for a millisecond time-scale spatial and temporal resolution. However, to construct such a channel in this way is more tedious biologically when compared to genetically expressing a rhodopsin channel in the specific area of interest (for example hippocampal neurons).

According to Karl Deissoroth et al [46] optogenetics is a new approach for these kinds of neuronal transmission studies. The growth of optogenetic methodologies has included the advancement of several approaches [46]: (1) one and two photon fluorescence microendoscopy for imaging fluorescently labeled cells deep within mammalian brain; (2) simultaneously imaging of mammalian functional brain maps and the dynamics of neuronal morphology in genetically targeted neocortical cells; (3) genetically targeted reporters for imaging subcellular biochemical function in living neurons; (4) mouse transgenic techniques for genetic control of biochemical function in fluorescently labeled neurons embedded within intact mammalian circuitry; (5) genetically targeted optical control of neural activity in behaving Drosophilia; and (6) high-speed, genetically targeted optical control of electrical activity in mammalian circuits.

The high-speed genetically targeted optical control of electrical activity has gained much importance as the next–generation optical technology for illuminating genetically targeted brain circuits due to the easily available and a simple system of two channels, ChR2 and NpHR.

1.6.2.1 ChR2 (Channelrhodopsin-2)

Ed Boyden et al. worked on a nerve protein that electrically excites (or depolarizes) the neuronal activity. ChR2 is found in green algae and is activated by blue light (wavelength ≈470nm peak). These channels could be genetically engineered to respond to light in specific cells (like the neurons). The green algae channelrhodopsin-2 could be used to control neuronal excitability. This channel depolarizes neurons up to a light stimulation frequency of 20 Hz [47]. The ability to light activate neurons via ChR2 is in the order of 1-20 ms [48]. The light power required to activate ChR2 is 5-12 mW/mm^2 [44].

1.6.2.2 NpHR (Natronomonas pharaonis)

Ed Boyden et al. searched for a complementary tool that would enable neuronal inhibition using a different wavelength of light. They found that targeting a light driven chloride pump halorhodopsin from the archaebacterium Natronomonas pharaonis to genetically specified neurons reliably silences them by millisecond-timescale pulses of yellow color light

(wavelength ≈ 590nm). The ability to light activate neurons via ChR2 is of the order of 1 millisecond. Hence we would want to have a complementary tool that has similar characteristics on the timescale as that of ChR2. NpHR provides the best solution amongst all the methods invented and discovered so far. Even brief pulsing of yellow light could completely silence the neurons and yet allow normal spiking activity within milliseconds [49].

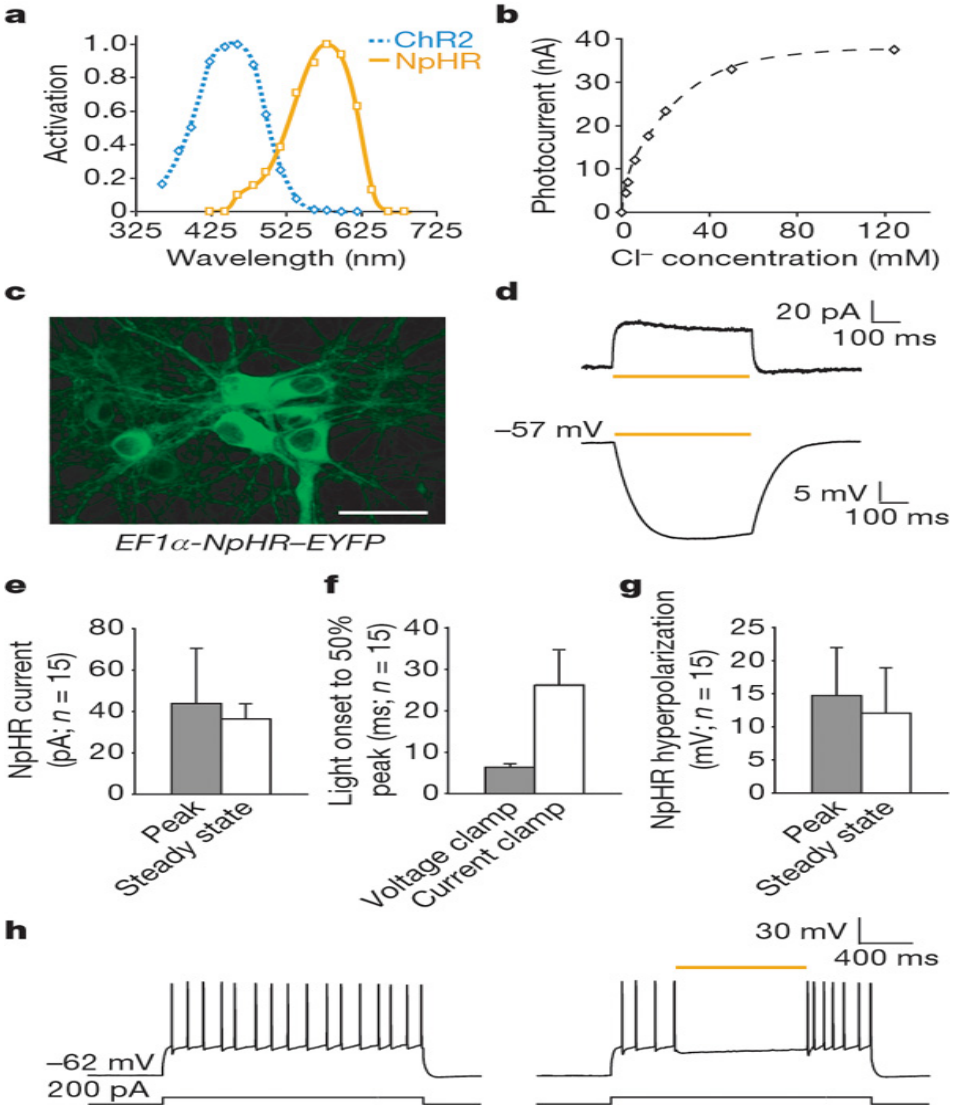

Figure 1.1 Electrophysiological properties of NpHR in oocytes and hippocampal neurons.

Figure Description: “a, Action spectrum of NpHR in oocytes held at 250 mV, determined by 20nm narrow bandwidth interference filters. The ChR2 action spectrum is provided for comparison4. b, Extracellular [Cl2] dependence of NpHR pump currents indicates a simple Michaelis–Menten type saturation with a KM of 16mM (dashed fit curve). c, Hippocampal neurons expressing NpHR–EYFP (scale bar 50 mm). d, Yellow light (593 nm)-induced outward photocurrent in neurons (top panel, voltage clamp) and membrane hyperpolarization (bottom panel, current clamp); illumination duration is indicated by the yellow bar. e, NpHR peak versus steady-state current (mean6s.d.; n515). f, Latency of NpHR activity measured from light onset to 50% of the peak current or hyperpolarization (mean6s.d.; n515). g, NpHR peak versus steady-state membrane hyperpolarization (mean6s.d.; n515). h, Illumination with yellow light potently inhibited neuronal firing.” Figure 1.1 was obtained from “Multimodal fast optical interrogation of neural circuitry” [51].

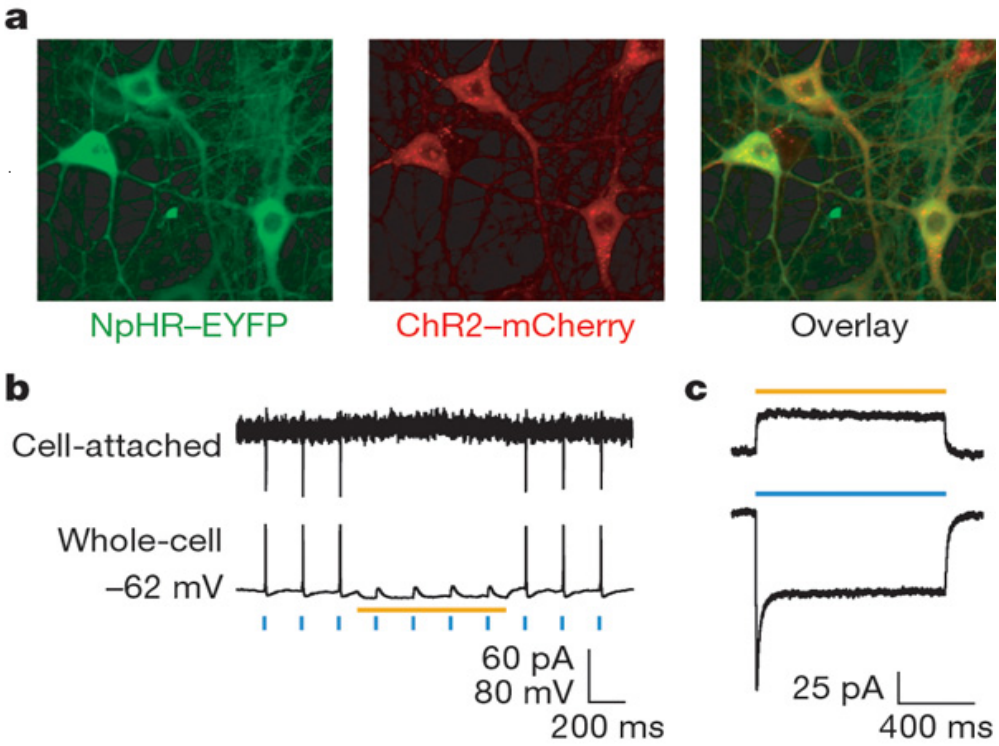

Figure 1.2 Combining NpHR with ChR2 for noninvasive optical control.

Figure description: “a, Hippocampal neurons co-expressing NpHR–EYFP under control of the EF1a promoter and ChR2–mCherry under control of the synapsin I promoter. b, Cell-attached and whole-cell recording of neurons co-expressing NpHR–EYFP and ChR2–mCherry. Action potentials are evoked by brief pulses of blue light (473 nm, 15 ms per pulse; length of blue bars is not to scale for ease of visualization). Simultaneous illumination with yellow light inhibited spike firing. c, Voltage-clamp recording from a single neuron co-expressing NpHR–EYFP and ChR2–mCherry, showing independently addressable outward and inward photocurrents in response to yellow and blue light, respectively.” Figure 1.2 was obtained from “Multimodal fast optical interrogation of neural circuitry” [51].

1.7 Simulating physiological conditions

Though simulating neuronal excitation is possible with tools such as ChR2 and glutamate uncaging, a closer complementary tool was not in existence until NpHR was discovered. Thus with NpHR, hyperpolarization could be achieved in synchrony with ChR2. NpHR is known as the “off” switch and on the other hand, ChR2 is known as the “on” switch. According to “multiple-color optical activation, silencing, and desynchronization of neural activity, with single-spike temporal resolution” [49], there are implications the NpHR channels may more accurately covey images from the outside world to the central nervous system. In the immediate future, the ability to study the effects of well-timed neuron or circuit inactivation in animal models of disease may rapidly reveal new principles for selecting neural circuit targets for treatment of specific disorders.

The paper predicts that the ability to optically silence neural activity in multiple kinds of organism using NpHR will transpire in quite short order. Also it says that the newly enabled system of driving excitation and inhibition of genetically targeted neurons with blue and yellow light will likely be particularly valuable for probing the role of specific subsets of neurons in neural computations. This statement has become the basis for this thesis work.

According to “Multimodal fast optical interrogation of neural circuitry” [50], NpHR/ChR2 system enables rapid bi-directional control of neurons on the timescale of milliseconds, thus enabling emulation or alteration of the neural code. Also, both NpHR and ChR2 can be functionally expressed and operate at high speed in the mammalian brain without necessitating cofactor addition.

1.8 Advantage of NpHR over RO4

A path breaking and pioneering earlier work demonstrated that neuronal circuits can be manipulated by expressing mutated ion channels or G-protein receptors (GPCRs). As an example, the regional expression of a genetically modified K^+ channel in Drosophilia was able to suppress the excitability of targeted cells i.e., muscle, neurons, photoreceptors [47]. According to Xiang Li et al [47], silencing of cortical neurons was achieved by binding of the peptide allostatin to its exogenously expressed receptor. Recently, Zemelman et al’s work, elegantly demonstrated that light activation of the protein complex, encoded by the Drosophilia photoreceptor genes (i.e., arrestin-2, rhodopsin, and G protein α subunit), could induce action potential firing of hippocampal neurons. Activation and de-activation of neuronal firing could also be achieved when ligand-gated ion channels, such as the capsaicin receptor, menthol receptor, purinergic receptors, or light controllable K^+ channel blockers, were used to control firing in hippocampal neurons. However, the application is limited as it is relatively slow when compared to physiological conditions.

To overcome these limitations, Peter Hegemann et al., came up with a molecular probe, vertebrate rat rhodopsin 4(RO4). This was used in conjunction with ChR2 to imitate synaptic transmission bi-directionally. The RO4 is a member of the vertebrate rhodopsin family that acts via the Gi/o pathway (Gi/o protein is a heterotrimetric G protein subunit which inhibits the production of cAMP from ATP [51] to reduce the excitability by increasing somato-dendritic K+ and decreasing pre-synaptic Ca2+ conductance in neurons. To depolarize these neurons, ChR2, a cation channel was used to produce a high Na+ conductance. Also, both act at a

millisecond time-scale that is very suitable and preferred method for studying neuronal transmission. This would facilitate in creating a system for synaptic transmission close to the physiological conditions. They worked well in cultured hippocampal neurons and then introduced into embryonic chick spinal cords where they shown to be capable of controlling spontaneous rhythmic activity in isolated cords embryos. Thus the newly obtained system will enable the researchers to probe into neuronal computations.

According to Ed Boyden et al. [52], NpHR is five to ninety times faster than RO4. This is very important considering the millisecond-timescale physiological neuronal transmission. It is worth noting here that all the ChR2 channels in the path of continuous light will be activated. However, the usage of pulsed light improves the resolution both spatially and temporally [47, 44].

1.9 Research problem

From the above sections, it is clear that the neurons can now be studied at various cellular and subcelluar levels due to the improvement in the spatial resolution. However, none of the techniques discussed above have the capability of stimulating the neurons selectively. The aim of this work is to “build an instrument that can target various cellular and subcellular components of neurons selectively in the field of view”.

Hypothesis Statement:

“The understanding of neurological communication and memory can be advanced through the construction, testing and optimization of a nanopatterning system capable of providing precisely timed light pulses at specific wavelengths matched to engineer light receptors”.

CHAPTER 2

MATERIALS AND METHODS

2.1 Preparation of genetically engineered neurons

The neurons have to be genetically engineered to respond to light in order to study the neural circuits on the nanopatterning system. Engineering these neurons required a set of tissue culture techniques which will be discussed in the following sections.

2.1.1 Plasmid

The plasmids required to genetically engineer neurons to respond to light were obtained by Dr.Joachim Herz (Dept. of Molecular Genetics, UTSouthwestern Medical Center) from Dr.Karl Deissoroth (M.D., Ph.D., Depts. of Bioengineering and Psychiatry, Stanford University) who is the pioneer in developing the technique of bidirectional control of neurons expressing ChR2 and NpHR channels. However, these plasmids were modified to encode lentivirus vector under the control of Ubiquitin promoter. This was accomplished keeping in view, the final goal of this project that is to use the nanopatterning system to study the neural network of living hippocampal brain slices. This is however, beyond the scope of the work discussed in this thesis. Tables 2.1 and 2.2 give a brief account on the plasmids.

Table 2.1 Original Plasmid from Deissoroth Lab, Stanford used as controls. Courtesy: Herz lab

Name	Description	Size	Notes
AAV-EFa-double floxed reverse-hChR2 (H134R)-EYFP-WPRE-pA (DIO)	For Cre mouse, pEF-1a	7.3Kb	Plasmid carries an Ampicillin Resistant gene, volume of plasmid increased using DH5 α stock

Table 2.2 Modified plasmid by Herz lab, UTSW used for expression in hippocampal neurons.

Name	Description	Size	Notes
FUGW: pUb-ChR2(H134R)-EYFP	Lentiviral expression Vector	10.6Kb	Plasmid carries an Ampicillin Resistant gene, volume of plasmid increased using DH5 α stock

2.1.1.1 Maintaining the plasmids

The volume of plasmid obtained from Herz lab was 20µl with a concentration of 7.4µg/µl. Since the quantity of the plasmid was not sufficient to carry out all the experiments, the plasmid volume had to be increased. For this purpose, DH5 α (donated by Kodadek Lab, DTR, UTSW) was used. The LB broth (from GIBCO BRL; catalog number: 12795-027; also referred to as Agar) solution was prepared and coated onto 100mm dishes (Corning CLS 430167). The coated plates were placed inside a plastic bag and flipped over so as to avoid condensation on the agar. On the next day, the bugs (DH5 α) were thawed from the -70˚ C freezer. The plasmid was added to the DH5 α cells and heat shocked for 40 seconds. LB+Amp solution was made and it was added to the DH5 α cells. The cells with the plasmid were then rescued at 37˚C incubator (Fisher Scientific Isotemp incubator; Model 655D) for 24 hours and spread at 50µl and 100µl concentrations on the Agar coated plates. Although, the incubator used neither has a CO_2 flow nor a water bath, it could serve the purpose as neither of them was required for the growth of DH5 α cells. A detailed description of the procedure for making the LB Agar plates, pouring the plates and a Transformation protocol for the DH5 α cells is given in Appendix C and Appendix D respectively. The plasmid DNA was then extracted and purified from the cells by using the QIAprep Spin Miniprep Kit and a microcentrifuge (eppendorf centrifuge 5417C). The protocol is detailed in Appendix B.

2.1.1.2 Sequencing the plasmid

The plasmids that were obtained from Herz lab were amplified using primers on PCR machines and sequenced to match with the sequence of the plasmid to be used for genetically engineering the neurons. The primers used were:

Seq 5^1 to 3^1: GGCAGCGCTGCCACCATGGATTATGGAGGCGCCCTGAGT (forward)

Seq 5^1 to 3^1: GGCACTAGTCTATTACTTGTACAGCTCGTC (reverse)

These primers were used for PCR amplification. The sequencing results were used to confirm for the ability of the plasmid to express ChR2 channels tagged with EYFP fluorescent dye.

2.2 Cell culture

Cell culture was done in the tissue culture room (Division of Translational Research, UTSW). The cells were maintained in the Forma scientific, Inc; CO_2, water jacketed Series II incubator. The cells were cultured in 100mm Corning petri-dishes (CLS 430167) for carrying out both transfection and infection of cells. However, infection required the usage of 6-well plates (35mm Falcon petri-dishes; Catalog number: 353046) apart from 100mm dishes. Two cell lines were maintained in the process of genetically engineering the neurons: 293T cells and Neuro-2A cell line. 293T cells were donated by Herz lab. Neuro-2A cell line was bought from ATCC (CCL-131^{TM}). The cells were cultured in DMEM with 4500mg glucose/L, 110mg sodium pyruvate/L and L-glutamine supplemented with 10% Fetal Bovine Serum (FBS) and 1% Penstrep (10000 I.U/ml penicillin and 10000 µg/ml streptomycin). Penstrep was bought from Cellgro (catalog number: 30-002-CI) and donated by Herz lab, Dept. of Molecular Genetics, UTSW. DMEM was bought from Sigma-Aldrich (catalog number: D6429) and FBS was bought from GIBCO (catalog number: 16000).The FBS was heat inactivated by heating to 56˚C for 30minutes prior to being mixed with the DMEM. This medium will henceforth be referred to as D10 for simplicity. PBS pH 7.4 (without calcium chloride and magnesium chloride) was used as a wash buffer while splitting and passaging the cells. PBS was bought from GIBCO (Catalog number: 10010-049). Trypsin EDTA, 1X (0.05% Trypsin, 0.53mM EDTA in HBSS without

calcium and magnesium) was used to passage the cells by aiding in the detachment of cells from the monolayer. Trypsin was bought from cellgro (catalog number: 25-052-CI) and donated by the Herz lab, UTSW.

2.3 Transfection of 293T cells

Lentivirus was produced by transfecting 293T cells (CRL-11268™) with the plasmid DNA. 293T cells were seeded in appropriate number of 10cm plates (using D10). Cells were seeded at a density of around 30-40% confluence in order for the cells to be 60-80% confluent by the next day. The cells were checked on the next day to see if 293T cells reached a confluency level of (60-80%). Once it reached the appropriate confluency, 293T cells were transfected. The transfection protocol is described below:

Transfection of 293T cell-line (Protocol-adopted from the protocol used by Graff Lab, UTSW):

A) Add 800µl of DMEM into a microtube.

B) Add 24µl of Fugene6 directly into DMEM avoiding direct contact of Fugene 6 reagent with the plastic surface of the microtube. Invert gently to mix contents. Incubate for 5 minutes.

C) Add 1.08 µl (8/7.4 µg/ µl) of plasmid into the diluted Fugene 6 reagent from 2). Invert gently to mix contents.

D) Incubate for atleast 15 minutes at room temperature (upto 45 minutes).

E) Change media for 293T cells plated on the previous day.

F) Add the transfection mix from 4) in a dropwise manner to the 293T cells seeded on the previous day. Gently swirl plate to ensure even dispersal of transfection mix.

G) Return plates to CO_2 incubator.

On the following day, the 293T cells that were treated for transfection were observed on an inverted Olympus IX 71 fluorescence microscope. Green colored fluorescence was observed using an 'ET/Sputtered Chroma EYFP' filter set (by Chroma; 49003 ET-EYFP filter set).The supernatant was collected under a tissue culture hood in a 50ml conical tube (BD Falcon; Catalog number: 352077) and filtered through a 0.22µm filter (by Millipore; Catalog number:

MPGL04001) attached to a syringe (BD 20ml Syringe; Catalog number: CI-XGX2-M17C) , in order to filter out the 293T cell contamination and store the concentrated virus. This virus will be referred to as ‘First Harvest’ for convenience. The supernatant that was extracted from the plates was replaced with ‘D10’ medium and the plates were restored to the incubator in the tissue culture room (DTR, UTSW). After 24 hours, the cells were once again observed for fluorescence on the Olympus IX71 inverted microscope using the ‘ET/Sputtered Chroma EYFP filter set. The test for fluorescence was positive and hence the supernatant from the plates was collected and the plates discarded. The supernatant was then filtered using a 0.22μm filter attached to a syringe and the virus concentrate was stored in a 50ml conical tube. This will be referred to as ‘Second Harvest’ for convenience. The ‘First Harvest’ and the ‘Second Harvest’ were mixed together and stored in a 50ml conical tube. This will henceforth be referred to as the ‘Final virus concentrate’. Figure 2.1 depicts the 293T cells viewed through an EYFP filter set on the fluorescence microscope.

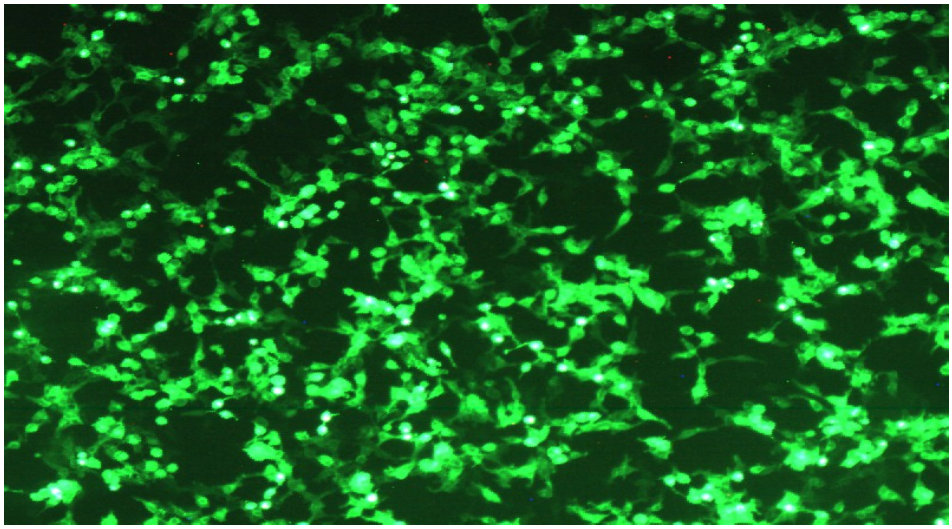

Figure 2.1 Lentivirus was produced from 293T cells to infect the Neuro-2A cell line and thus express the channels

2.4 Neuro-2A cell line

The Neuro-2A cell line was bought from ATCC (catalog number: CCL-131^{TM}). These cells were used as the final target cells to achieve selective control of neurons. Neuro-2A cells are obtained from mouse brain and hence they do not possess the inherent capability to respond to light. Hence, they had to be genetically engineered to respond to light. The procedure followed to achieve this is described in the following sections.

2.4.1 Infection of Neuro-2A

On the day of the 'First Harvest', the Neuro-2A cells were plated in appropriate number of 10cm plates (in 'D10') at a confluency of 20-25% so that they reached a confluency of 40-50% by the next day. On the following day, the cells were observed for appropriate confluency for infection. The test results were positive. Polybrene (10mg/ml stock) was added to a final concentration of 5µg/ml to the 'Final virus concentrate'. The existing media on the cells was aspirated and the 'Final virus concentrate' containing polybrene was applied to the cells. The plates with the cells were then returned to the incubator at 37˚C in the tissue culture lab (DTR, UTSW) for 24 hours. The viral concentrate was then aspirated and replaced with 'D10 media and the cells were returned to the incubator. Trans-gene expression was analyzed 72 hours post infection. However, there was no sign of infection though some fluorescent debris was found in the Petri-dish. The whole procedure of infection was repeated several times to eliminate errors. The infection was however not a success. Hence, the Neuro-2A was directly transfected with the plasmid to genetically engineer them to respond to light. The details of the transfection procedure are discussed in the next section.

2.4.2 Transfection of Neuro-2A

The Neuro-2A cells were seeded in appropriate number of 10cm plates in 'D10' medium. Cells were plated at a confluency of 30-40% so that they would be 60-80% confluent (considered to be optimal for Fugene 6 transfection) the next day. The following day, cells were

checked for the appropriate confluency for transfection. The transfection protocol used was similar to 293T transfection. The protocol is detailed below for Neuro-2A.

Transfection of Neuro-2A (Protocol-adopted from the protocol used by Graff Lab, UTSW):

A) Add 800µl of DMEM into a microtube.

B) Add 24µl of Fugene6 directly into DMEM avoiding direct contact of Fugene 6 reagent with the plastic surface of the microtube. Invert gently to mix contents. Incubate for 5 minutes.

C) Add 1.08 µl (8/7.4 µg/ µl) of plasmid into the diluted Fugene 6 reagent from 2). Invert gently to mix contents.

D) Incubate for atleast 15 minutes at room temperature (upto 45 minutes).

E) Change media for Neuro-2A cells plated on the previous day.

F) Add the transfection mix from 4) in a dropwise manner to the 293T cells seeded on the previous day. Gently swirl plate to ensure even dispersal of transfection mix.

G) Return plates to CO_2 incubator.

The cells were observed under an Olympus IX 71 inverted fluorescence microscope for transfection efficiency. These cells were not 100% transfected. However, it would still be possible to analyze the interconnections within the transfected groups of neurons. Hence sub-cloning, to achieve 100% transfection was not done. Figure 2.2 shows the ChR2 expression made visible by tagging it to the EYFP fluorescent dye.

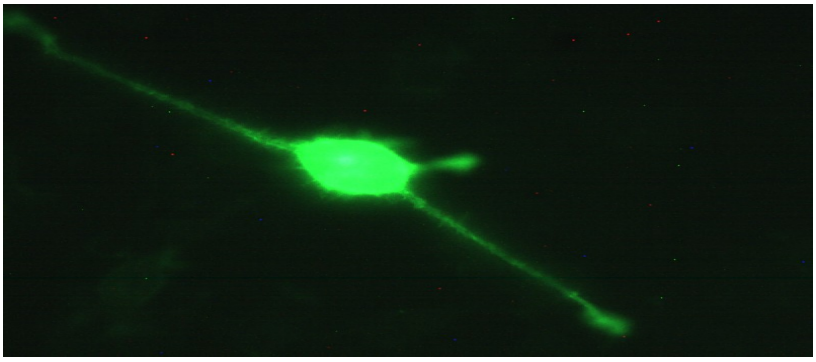

Figure 2.2 The Figure depicts the transfected neuron at 40X objective power. Lentiviral infection of Neuro-2A did not express the channels. ChR2 channels tagged with EYFP were expressed by direct transfection of Neuro-2A cell line.

2.5 Slowing the rate of photobleaching

Two techniques were implemented to reduce the rate of photobleaching: Neutral density filters and a chemical called Trolox (by Sigma-Aldrich; catalog number: 238813-5G). Neutral density filters with various optical densities were used to reduce the rate of photobleaching. However, the intensity from the mercury lamp was high enough to cause significant photobleaching even with the darkest density neutral filter available in the Garner lab. Hence, a chemical compound called Trolox was used to achieve this. The chemical name of this compound is 6-Hydoxy-2, 5, 7, 8-tetramethylchroman-2-carboxylic acid with a molecular formula of $C_{14}H_{18}O_4$. This chemical was used as an antioxidant to keep the cells from photobleaching during imaging. Trolox is a cell-permeable, water soluble derivative of vitamin E with potent antioxidant properties. It prevents peroxynitrite-mediated oxidative stress and apoptosis in rat thymocytes. Since, live cells were used in this work; the solvent used for Trolox was water (maximum solubility of 0.5mg/ml) instead of ethanol (maximum solubility of 160mg/ml).

2.6 Fluo-3/AM

Fluo-3/AM is a non-ratiometric calcium imaging dye. Membrane-permeant form and thus can be loaded into cells via incubation. Fluo-3/AM itself does not bind Ca^{2+}, but it is readily hydrolyzed to fluo-3 by endogenous esterases once the dye is inside the cells [54]. It is an Orange red solid soluble in DMSO and has to be kept frozen at -20℃. It has to be protected from light, especially when in solution. Fluo-3 was used in the place of Fura-2 (ratiometric dye) to conduct preliminary testing of calcium activity when the neurons are stimulated. The results are discussed in Chapter 4 of this document.

Chemical Formula: $C_{51}H_{50}Cl_2N_2O_{23}$

UMWU filter cube on the Olympus microscope was used to view Fluo-3.

2.7 ACSF (Artificial Cerebro Spinal Fluid)

Artificial Cerebro Spinal Fluid was used in the experiments to increase the amount of extracellular calcium. The calcium activity readout requires the extracellular calcium to enter the cells and bind to the fluorescent dye upon application of the stimulus. The cells are bathed in ACSF since the experimental conditions are not natural and require the presence of artificially induced extracellular calcium in the petri-dish.

2.8 System Design

Two technologies were integrated to build the Nanopatterning system. The Digital Light Processing system by Texas Instruments and the Olympus IX71 inverted epi-fluorescence microscope. These two technologies were integrated using integrating optics. The spatial control achieved using this system is unprecedented. A third technology referred to as NI LabView by National Instruments was integrated into this system to add the dimension of temporal control in the system. The conceptualization of the system, the design and integration of these three technologies is described in this part of the thesis.

2.8.1 DMD and Video cards

DMD is used to modulate the pattern with light to generate a light pattern that can accurately target the selected structures. The pattern is generated by taking a picture and converting it to a gray scale image. This gray scale pattern is then sent to the DMD using a set of video cards, custom designed for the purpose of interfacing the DMD with the computer.

2.8.1.1 DMD

The Digital Micromirror Device (DMD) is the heart of the system. The DMD used in the system consisted 786,432 micromirrors arranged in a 1024 x 768 matrix. Each mirror was a 16µm x 16µm square with a spacing of 1µm between mirrors. Each mirror of the DMD chip was programmed to tilt to either a + 10 degree or – 10 degree position depending on the binary state of the SRAM cell that exists below each mirror. Each individual mirror controls the mirror position using SRAM data stored in the SRAM cell below. The SRAM cell consists of

binary data. Thus the mirror is considered to be operating in an electro-mechanical way. The position of a DMD mirror that reflects UV light to the target is defined to be in ON state and the position that reflects light away from the target as the OFF state. The different positions of the individual mirrors determine the direction in which the light is reflected.

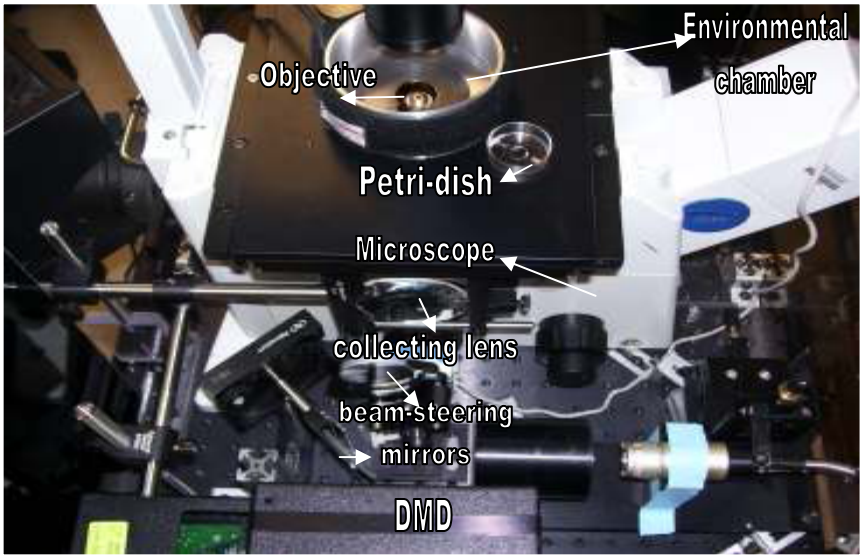

Figure 2.3 The figure shows the DMD with the microscope and the integrating optics. The DMD is connected to the CPU via a set of video cards that transmit the gray scale pattern to the DMD. The Petri-dish, objective, beam-steering mirrors and collecting lens are also indicated to depict the light path from DMD to the Petri-dish.

The reflection from all the mirrors together creates a specific image pattern of the wavelength of light incident from the source. Thus a pattern of light can be generated that can be spatially modulated using the DMD. Control of the illumination and collection of the cone of the pattern is accomplished by using a lens to focus this pattern of light onto the bottom of the petri-dish as shown in Figure 2.3.

2.8.1.2 Video cards

The PCI card of the electrical sub-system consisted of External connectors that included Universal PCI-connector (3.3 V & 5.0V PCI slots), CRT connector or plug and display connector, 100-pin half pitch LCD connector, 40 pin YUV Direct Video Input port, USB Pass

through connector and PanelLink Power connector. The card also consisted of an EMI suppression filter on analogue CRT signals. It took a supply voltage of 5.0V ± 5% and its operating temperature range was 0-60℃.Power dissip ation was approximately 3-6W.typ and its dimensions were 174mm x 107mmx 18.3mm [55].

The XGA class of DMD product requires a digital video interface from a computer system. The commercially available video card consists of a PanelLink Video card. The PanelLink output is not used due to excessive pixel clock noise; instead the direct digital outputs are used to interface with the XGA Video Driver Card. The XGA Video Driver Card connects to the XGA Video Receiver Card via a SCSI III cable. In turn, the XGA Video Receiver Card will mate to either the DMD Formatter Board or the Unit Under Test (UUT).

2.8.2 Epi-fluorescence Microscope subsystem

Olympus IX71 inverted microscope was used to observe the fluorescence of the two channels. It has a filter turret that can hold six filter cubes. A hole was made in the filter turret and a side cube was used to direct the pattern of light projected from the DMD onto the bottom of the Petri-dish. The integration of the DLP sub-system with the epi-fluorescence microscope is described in Chapter 3.

2.8.3 NI LabView software

NI LabView 8.5 student edition software by National Instruments was used to control the strobe lamps, SenSys camera, the filter wheel and the display of images to be transmitted to the DMD chip. IMAQ Vision 8.6.1 Development Module also by National Instruments was used in conjunction with NI LabView 8.5 for image display.

2.8.4 Light Sources

Various light sources were used to provide different wavelengths of light to the system for control/manipulation of neural circuits. Each light source has a different lamp with different characteristics. The purpose of using each light source and their characteristics are described below.

2.8.4.1 Pulsed Light sources

X1200 strobe lamps by Perkin Elmer were used to flash pulsed light to affect the ChR2 and NpHR channels in the specimen with blue and yellow wavelengths of light. The flash rate of these lamps is 20Hz. Hence it the pulse repetition rate was set at a maximum rate of 20Hz and the system was not operated faster than this set point. The xenon lamps used allow a light output flash duration of 8-10microseconds. Table 2.3 depicts the pinout connections that were used to trigger the strobe lamp with TTL pulses. From the Table 2.3, it is clear that pin 4 and pin 5 are the negative and positive inputs of TTL pulses respectively.

Table 2.3 The Table depicts Signal Input Connector - J2 of the strobe lamp. The highlighted pin connections are the pins that were used to trigger the strobe lamp. Pin 4 was used as the ground and Pin 5 was used as the positive trigger input to the strobe lamp.

Pin 1	No connection
Pin 2	Internal Vref (voltage reference) output
Pin 3	External Vref (voltage reference) input
Pin 4	Trigger: opto-isolator trigger return
Pin 5	Trigger: opto-isolator trigger input
Pin 6	No connection
Pin 7	Chassis ground
Pin 8	Chassis ground
Pin 9	Vref (Voltage reference) return

For its operation, an external trigger input with electrical parameters of +5V TTL pulse, 20mA, 10-100microseconds is provided by the digital control board combined with the NI LabView program. Figure 2.4 depicts the X1200 strobe lamp. X1200 strobe lamps were modified to flash blue and yellow wavelengths of light. To achieve this, the housing of the lamps was taken apart. The face plate of the lamps with an aperture for interfacing the fiber optic cable with the lamp was mechanically altered to accommodate the filter. The filter was installed on the inside of the

face plate of the lamp. The housing of the lamp was then fixed back. An adapter was installed on the outside of the face plate of the lamp to interface it with the fiber optic cable. Henceforth, the strobe lamp that was installed with blue filter (FB 470-10 by Thorlabs) will be referred to as 'blue strobe lamp' and the strobe lamp that was installed with the yellow filter (FB 580-10 by Thorlabs) will be referred to as 'yellow strobe lamp' henceforth.

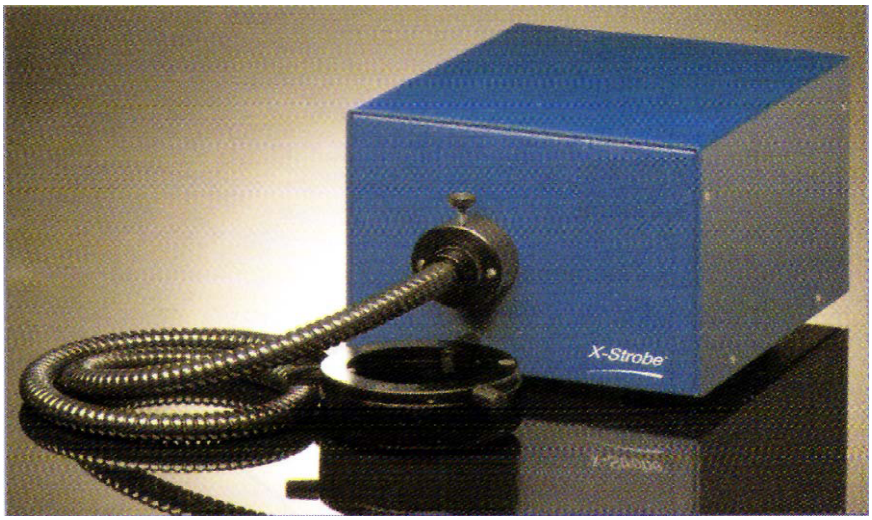

Figure 2.4 X1200 strobe lamp by PerkinElmer [59]. The Xenon lamps in the source were used to provide pulsed light to the system. The triggering of the strobe lamp was controlled using an external digital board called USB-6008.

As mentioned above, two filters were used to achieve blue and yellow wavelength pulsing. The filters allow 470nm and 580nm wavelength filters respectively. Thus, the actual intensity of light leaving the strobe lamp depends upon the transmission characteristics of both the pulsed light sources and the respective filters mechanically installed in them.

2.8.4.2 UV light source

Lightning Cure 200 UV spot Light source (Model No #7212-01) was used for Fura-2 calcium imaging readout. It is used as a continuous light source with the wavelength switching provided by the filter wheel. The UV light is allowed to pass through the filter wheel and then transmitted through one of the fiber optic cable branches to the optical sub-system. Figure 2.5 represents the UV lamp used for Fura-2 measurements.

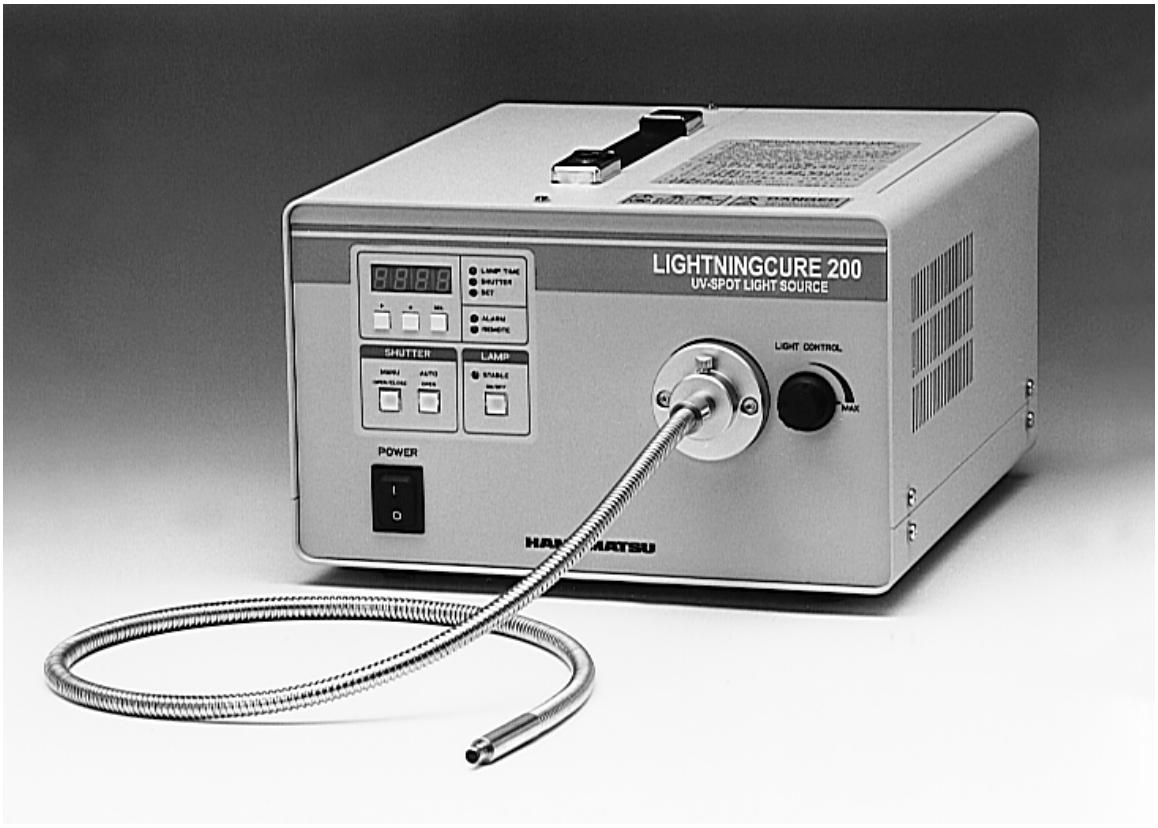

Figure 2.5 The figure represents the UV light source with the fiber optic guide. The UV source was used for Fura-2 measurements that require exposing the specimen to 340 and 380nm wavelengths of light. The fiber optic cable is removed and a filter wheel with 340 and 380nm filters installed and positioned in front of the aperture of the cable adapter.

2.8.4.3 Oriel Lamp

The Oriel 1000W Hg (Xe) lamp was used to provide higher intensity of light. However, as shown in the figure, at 470nm and 580nm, the intensity of light is around 100W and thus the lamp could not provide enough intensity to trigger the channels.

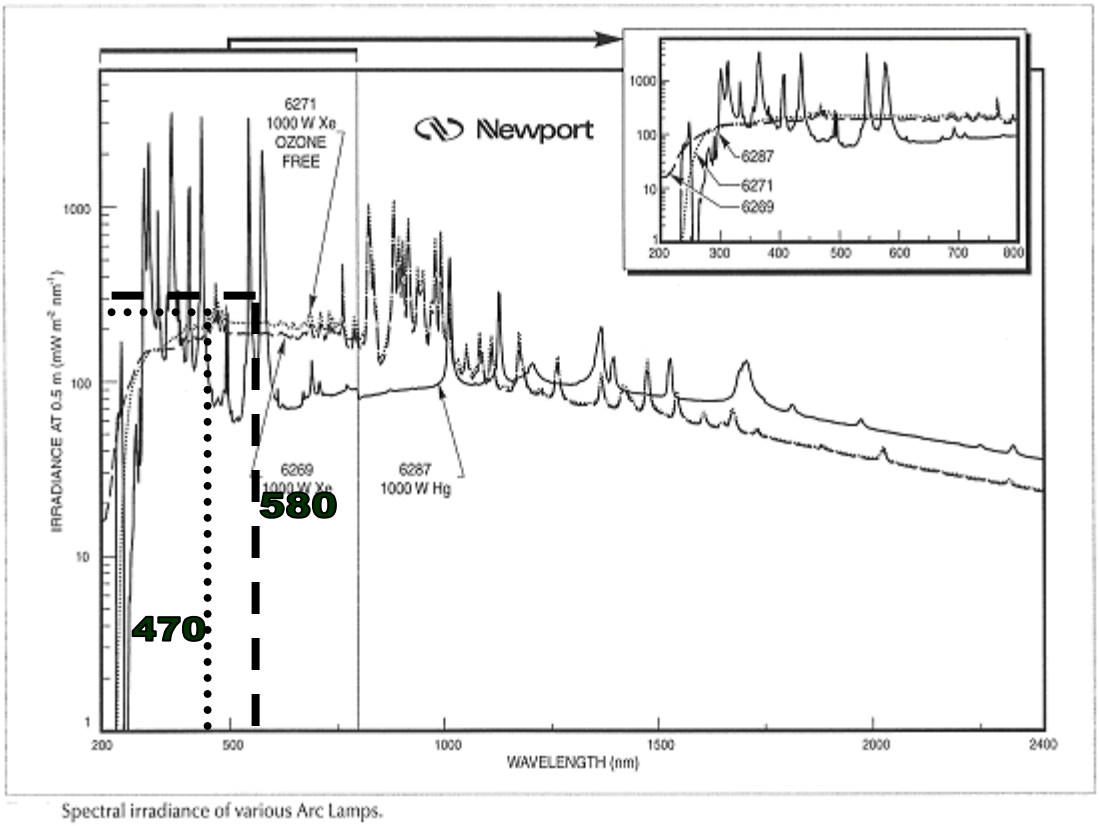

Figure 2.6 The figure depicts the spectral characteristics of the 1000W Oriel lamp used on the system to improve the intensity of light reaching the specimen. The spectral characteristics at 470nm and 580nm are clearly marked. These are the wavelengths at which the channels can be triggered.

Oriel lamp was used to get increased intensity of light at the output. It uses a Hg (Xe) lamp. However, the lamp could not provide the required amount of intensity to trigger the channels. As seen in the Figure 2.6, the intensity at 470nm and 580nm is not sufficient to trigger the channels. The intensity of light reduces to a large extent as it reaches the specimen.

2.8.5 Camera and Image Acquisition

Two cameras are used for acquiring images in controlling/manipulating neural circuits. Motic camera is used to locate the channels in a given specimen and SenSys camera is used to image the calcium activity readout. SenSys camera is used over Motic camera for calcium activity because of the 12-bit dynamic resolution of the SenSys camera which allows for

recording subtle changes in intensity. The cameras and their characteristics are as described below.

2.8.5.1 Motic camera

Figure 2.7 The Figure depicts the Motic CCD camera used on the system. The USB camera is used to locate the channels in a given specimen.

Motic M2000 is 2.0 Mega pixels with USB 2.0 PC output digital camera. The still image resolution of the camera is 1240 x 1024. The desired number of pixels can be set using the camera software settings. It is used to obtain images representing true color while eliminating interference and noise completely using the special “Background Calibration” feature. This is a ½” CMOS camera. Specifications for the Motic camera from the manual are given below in the Table 2.4.

Table 2.4 The Table summarizes the specifications for Motic Digital camera. The camera is generally run at 10fps to acquire higher resolution images.

Specifications for Moticam Digital Camera

Particulars	Moticam 2000
Image Device	1/2" CMOS
Lens	16mm
Effective Pixels	1600 x 1200
Still Image Resolution	1600 x 1200
Scanning System	Progress scan mode
Frame Rate	10fps @ 1600 x 1200; 40fps @ 800 x 600
Data Transfer	480MB/ second
Minimum Illumination	3 lux
Lens Mount	C-mount
Shutter	Automatic-Manual S/W Control
Video Output	Transmission across Motic software direct into memory of PC
White Balance	Automatic
USB Output	Yes
USB Power Supply	5V self-power from computer
Microscope Adapter	28, 30, 34 & 35 mm eyepiece couplers + B & S eyetube adapter
USB standard	2.0

When the Motic Images Plus 2.0 ML is run, workspace is displayed. In order to view the specimen image in real time, the capture window button is clicked. A screenshot of the capture window is shown as in Figure 2.10. The control panel can be used to change the quality and effects of the preview image. The gain, exposure, sharpness operations can be adjusted through slider bars to obtain the best quality images. ‘Capture’ is used to capture the real time image in the preview window. This image is saved in a temporary folder. The user can then save it elsewhere permanently as .JPEG images. The ‘Autocap’ confers upon the user the

ability to automatically capture series of images at specified intervals of time for a given amount of time. The camera software also enables users to record a movie by clicking on ‘Video’.

2.8.5.2 SenSys camera

Figure 2.8 Photometrics SenSys camera. It is used in calcium activity readout since the camera has a 12-bit dynamic range that can record subtle changes in calcium activity. [61]

SenSys® is an air-cooled camera system with the ability to acquire low-light images by integrating (exposing) over long periods of time. The imager in the camera is a scientific-grade charge-coupled device (CCD). It is a 12-bit CCD camera which has a high-speed shutter that maintains a speed of up to 15 frames per second while still fully opening and closing. The shutter takes 5 ms to open and 10 ms to close. The camera integration time (the total time any part of the CCD is exposed) is equal to the shutter open and close times plus the exposure time. Since it can detect 4096 levels of gray, this camera was preferred over the Motic camera for fura-2 imaging which requires identification of subtle differences in intensities. The camera functions in various modes like the ‘Timed mode’, ‘Variable-timed mode’, ‘Trigger First mode’, ‘Strobed mode’ and ‘Bulb mode’. In timed mode, the duration of each exposure time as well as non-exposure time of CCD array is constant throughout. Whereas for a variable timed mode this

duration varies and only time between two exposures remain constant. In ‘Trigger first mode’, the camera begins exposure only after external trigger pulse is given and then continues exposure sequence like in ‘Timed mode’. In ‘Strobed mode’, for every external trigger pulse an exposure takes place but each exposure sequence is of constant duration. For ‘Bulb mode’, each exposure sequence lasts until duration of each trigger pulse.

Table 2.5 The Table shows the pinout specifications of the SenSys camera. Pin 6 and Pin 9 were used as the positive and negative control of the camera respectively.

Pin #	Signal Name
1	+5V DC
2	+5V DC
3	Ground
4	Ground
5	Ground
6	+15V DC
7	Ground
8	-15V DC
9	Ground

.The camera is operated in strobed mode in this work. The Pinout specifications are described in Table 2.5. Pin 6 and Pin 9 were used as the positive and negative controls respectively. This is because the trigger pulses vary continuously for each experiment. The code for controlling the camera was written in Visual Studio by Dipen Rana, Garner lab, UTSW. NI LabView was used to call the executable and the camera was triggered.

2.8.6 Filter wheel and controller

The Filter wheel and controller were required for switching between 340nm and 380nm wavelengths of light. The two wavelengths are required for the ratiometric quantitative analysis

of Fura-2 readout. For filter switching, FW103S by Thorlabs was used. This combines the FW103 filter wheel with the TST001 T-cube stepper motor controller. The controller was software timed using NI LabView which controlled the filter wheel through the controller via an APT (Advanced Packaging tool). The filter wheel has a switching time of 250ms and can hold upto 6 filters.

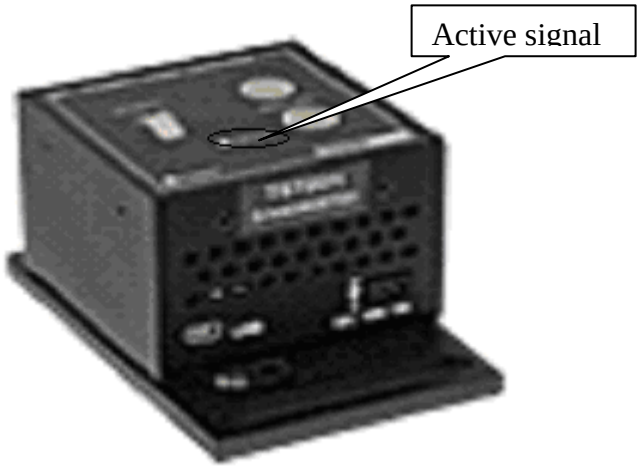

Figure 2.9 The Figure shows the TST001 filter wheel controller. The controller was used to control the filter wheel that has the 340 and 380nm filters fixed into it. The controller is called by an APT from NI LabView. The 'blinking' green light on the 'Active signal' indicates that the filter wheel is currently being controlled by the controller.

Figure 2.10 The figure shows the FW103S Filter wheel. The 340 and 380nm filters are installed on it. The movement of the filter positions is controlled by a controller which is in turn controlled by an APT that is called as a sub-routine from NI LabView.

As shown in the figures 2.9 and 2.10, the filter wheel is controlled by the controller. Both of them were bought from Thorlabs. The filter wheel controller was used to control the filter wheel. An APT program was supplied by Thorlabs along with the filter wheel controller. The APT sub-routine was called by NI LabView.

Table 2.6 The table summarizes the specifications of the filter wheel. The Step angle is used to move the position of the filter with respect to the filter wheel. The transition time between two filters is 250ms which is a limiting factor for calcium imaging.

Step Angle	1.8° (50 poles and ±2 phases for 360° divided by 200, or 1.8°)
Step Accuracy	5%
Rated Phase Current	1A
Phase Resistance	4.6 Ω
Phase Inductance	10.6mH
Holding Torque	23.1N.cm
Detent Torque	1.7N.cm
Phase Inductance	10.6mH
Operating Temperature	-20℃ to +40℃ (Motor Specifi cation Only)
Transition time between filters	TST001 Driver: 250ms

The angle by which the filter rotates is hardwired in the NI LabView program. As shown in the Table 2.6, the minimum step angle is 1.8°. The 340 nm and 380nm filters are positioned at 60 and 120 degrees respectively. The minimum transition time between two filter position with respect to the filter wheel is 250ms. This limits the rate at which the calcium activity readout could be imaged.

2.8.7 Digital control board

The Digital control board is used as an interface between the NI LabView software used to time the controls and the equipment being controlled. TTL pulses are given to the pulsed light sources and the SenSys camera to control them. The filter wheel does not need controlling through the USB-6008 digital control board as it is controlled by the filter wheel controller. The other event that requires timing is image display. However, this event does not require controlling through the digital control board. The IMAQ Vision development software controls the image display. Hence, the USB-6008 control board is used only to control the pulsed light sources and the SenSys camera.

2.8.7.1 Interfacing with the pulsed light sources

Figure 2.11 The Figure depicts the NI-USB 6008 that was used as the Digital control board to provide TTL pulses to the strobe lamp and the SenSys Photometrics camera. [60].

NI USB-6008 has 8 analog inputs (12-bit, 10 kS/s) and 2 analog outputs (12-bit, 150 S/s). It has 12 digital I/O [60]. The 32 bit counter that used to exist on the device was removed to make the device affordable. Hence it is to be noted that all the timing controls required for temporal control are software timed rather than hardware timed. The hardware

timing would have yielded better timing control. The device is bus-powered for high mobility and has built-in signal connectivity. It is compatible with NI LabView, Labwindows/CVI, and Visual Studio. NET. The digital board puts out only 8.5mA of current, which is not sufficient to trigger the strobe lamps. Hence, an amplifier was built to amplify the current to 20mA.

2.8.8 CPU

A T3400 CPU was used to control the software timing of the system. It is a 64-bit computer workstation. However, a 32-bit operating system was installed to run the computer as NI LabView 8.5 and the supporting software is 32 bit. It supports dual native PCIe X16 graphics slots for dual monitors. Thus PCI cards for SenSys camera and DMD video cards could be installed in this computer. An external power supply was connected to the DMD video card to run the card efficiently.

Figure 2.12 The Figure shows the Dell T3400 Workstation system. This system was chosen as it can accommodate all the PCI cards required to control the nanopatterning system. However, the installation of DMD video cards in the system reduced the rate of image display.

Summary of PCI Slots:

2 PCI-e x16 graphics slots

1 PCI-e x8 slot wired as x4

3 PCI 32bit/33MHz slot with support for 5v cards

2.8.9 Fiber optic cable

An Oriel 77536 Trifurcated glass bundle was used to deliver light from three different sources. Adapters (from Thor labs) were installed at the end of each branch of the fiber optic cable. Also, an adapter was mechanically installed on the other end of the fiber optic cable to interface it with the optical sub-system. Each leg of a trifurcated bundle receives 27% of the total incident radiation (approximately 4% is reflected at the input and output and packing fraction is 0.9). The transmittance at 470nm and 580nm is of particular interest. It is around 45-50%. This fiber optic cable however does not transmit UV light for fura-2 measurements. The fiber optic cable discussed here can be used for fluo-3 measurements which gives a qualitative measure of Calcium unlike fura-2 which is quantitative. A custom made fiber optic cable for fura-2 measurements from Oriel is being considered.

2.8.10 Environmental chamber

An aluminum environmental chamber wrapped with a thermal heating pad was used in order to maintain the optimum environmental condition for live cells. The thermal pad was used to provide temperature control (part number 2001 Model VI Kendrick Astro instruments, Canada).A flow gas control was also added to this setup and mounted to the microscope stage. The diameter of this stage is 10cm and its height is 5cm. A close fitting plexiglass lid contains two holes to which gas is flowed to maintain optimal life support conditions for live cells. The temperature control system can warm the petri-dish of cells in the environmental chamber to a maximum of approximately 42C. The experiment will be conducted at 37C, as required by the mammalian cells. In order to maintain the 5% CO2 environment required by the mammalian cell culture, a Blood gas mixture (5% CO2+21%oxygen+74%nitrogen) (Airgas incorporated (UN 1956)) will be used. A gas pressure regulator is used to adjust the gas flow rate [56].

2.8.11 NI LabView program

NI LabView could be used both to generate and acquire data. In this work, NI LabView was solely used to generate data. The functions are written in terms of VIs (Virtual Instruments).

This program is an integration of several functions. Each function is dealt with separately in the following sections:

2.8.11.1 Controlling the pulsed light sources

The pulsed light sources are controlled through a set of TTL pulses. The pulses are put out through a digital control board controlled through the NI LabView program. The screenshot of the program and the flowchart that describe the flow of the program are given below.

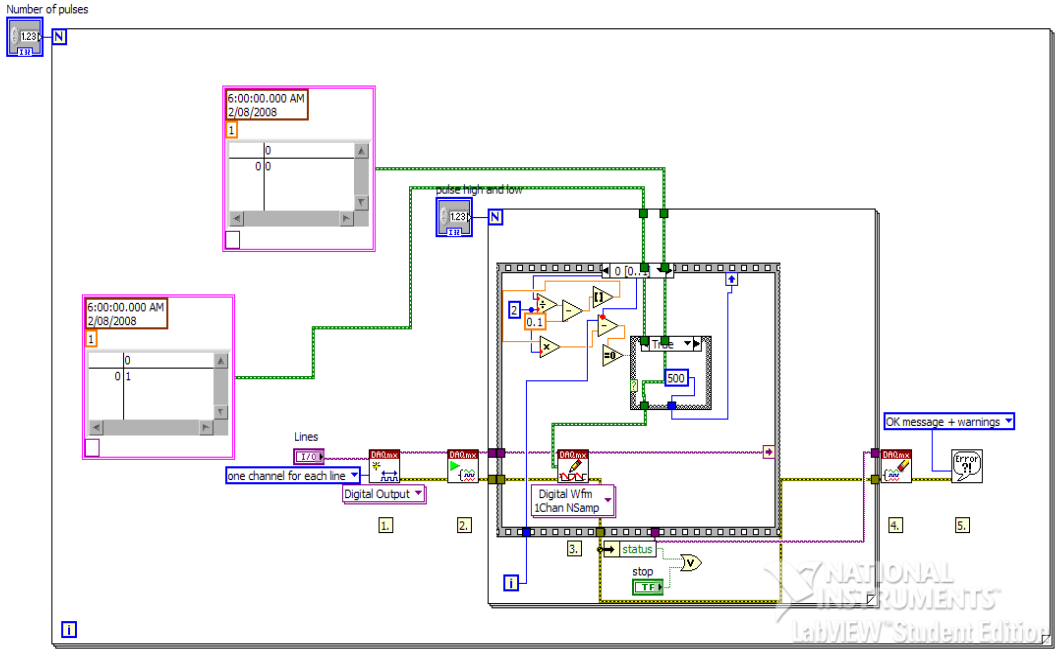

Figure 2.13 The Figure depicts the program to control the triggering of the strobe lamps in NI LabView. The program initially sets the waveform to digital output. The next VI starts the task and writes the digital waveform onto the channels that are hardwired into the program. The 'cleartask' VI clears the waveform from the memory.

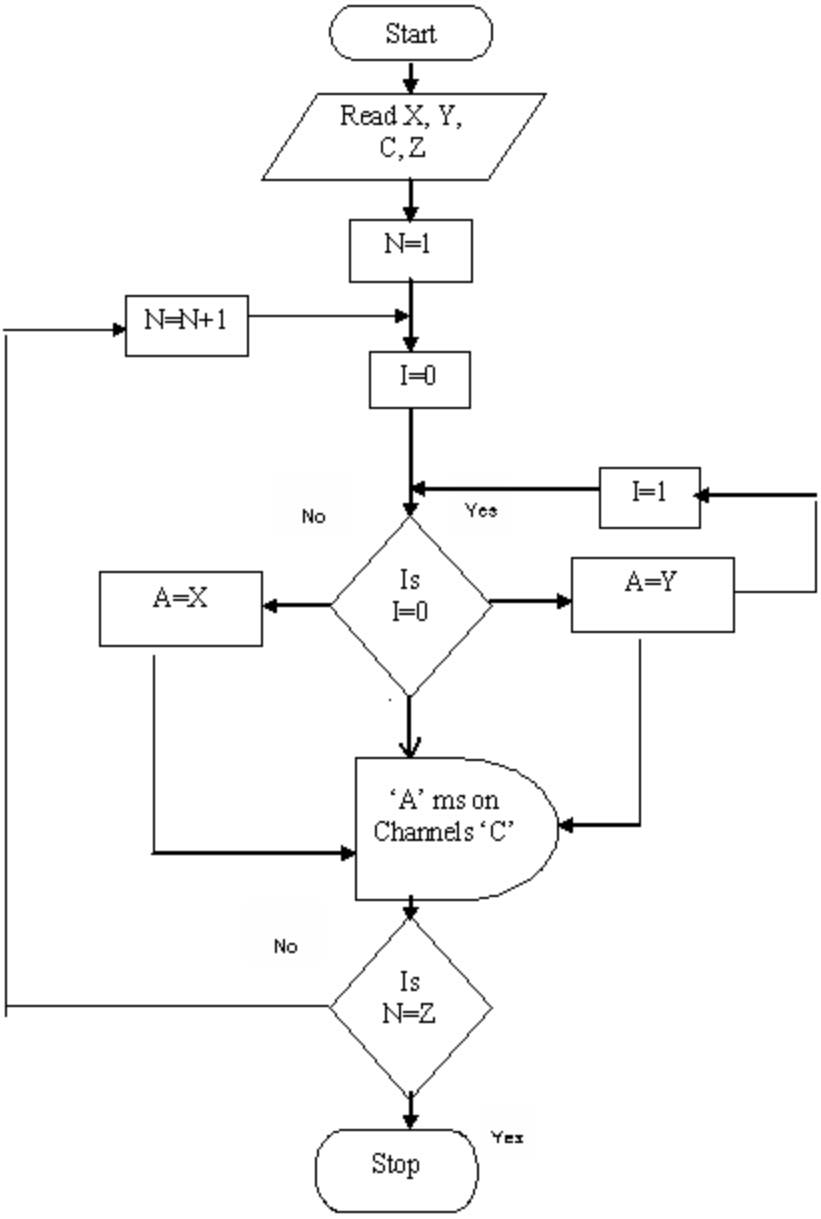

Figure 2.14 The figure depicts the flowchart for providing TTL pulses to the strobe lamps. The pulses are delivered in the form of a series of 'high state' and 'low state', held in that state for a particular period of time hard wired in the program. The channels on which the pulses have to be put out are also hard wired in the program.

In the above flowchart, ‘X’ and ‘Y’ represent the ‘off’ and ‘on’ states respectively. ’Z’ represents the number of pulses in the pulse train. The screenshot depicts the program to control the pulsed light sources. The program consists of a series of VIs connected to each other through wires to describe the flow of the program. The waveform is generated and then written on the specified channels on the Digital control board. The amplifier amplifies these signals and sends them to the strobe lamp which is then triggered.

2.8.11.2 Controlling the Display of images

The display of images has to coincide with the pulsing of the strobe lamps. This is to ensure that the image pattern and the light are modulated to produce a patterned light that can be used to spatially control/manipulate the neural circuits. The image display is controlled through the IMAQ vision development software. The screenshot of the program and the flowchart describe the flow of the program.

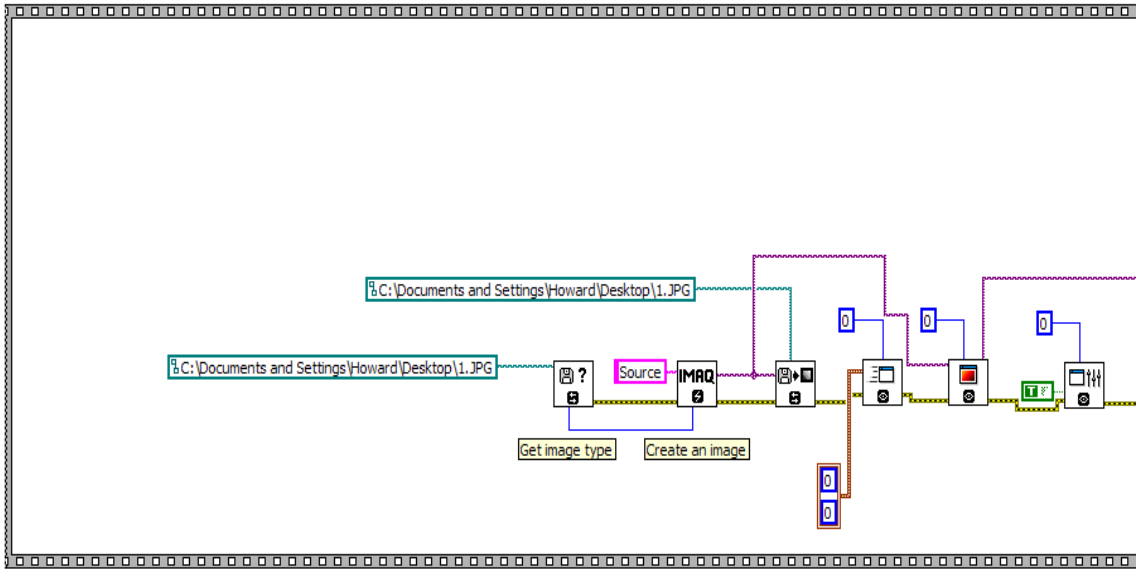

Figure 2.15 The Figure shows a part of the program that displays images. The image is read from the file and the window adjusted to fill the entire screen. The borders of the image window are removed.

The above program is used to display the images on the monitor. The figure 2.15 describes the flow of the program. The images are extracted from a file where the images are stored and adjusted to the window size of the monitor and displayed on the screen. The DMD video cards project these image patterns on the DMD.

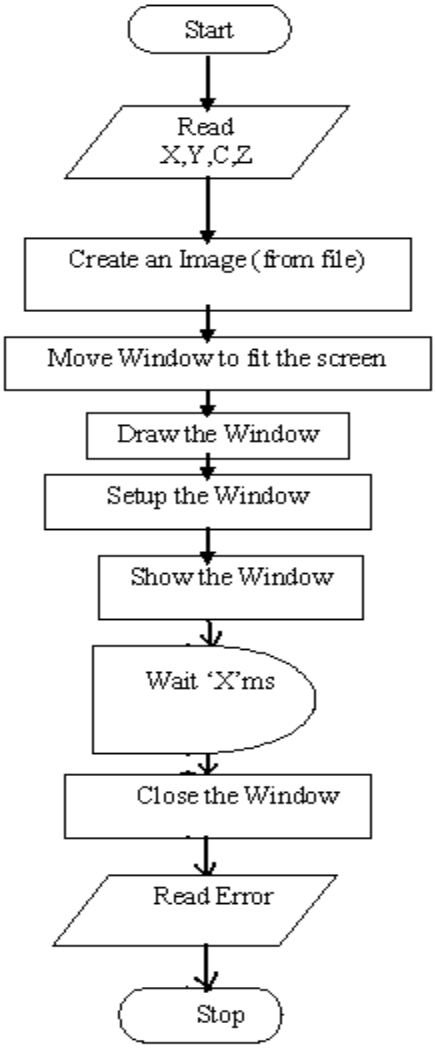

Figure 2.16 The Figure depicts the flowchart of the program that displays images. The image file and type are read, the image window is drawn, the image window is setup, the window is shown for a particular period of time (hardwired) and then the window is closed.

2.8.11.3 Controlling the filter wheel and controller

The filter wheel and controller are controlled by an APT through NI LabView program. The filter wheel has six filter positions. The 340nm and 380nm filters are fixed to the filter wheel. The movement of the filters with respect to the filter wheel is controlled using the program. The screenshot of the program and the flowchart given below describe the flow of the sub-routine.

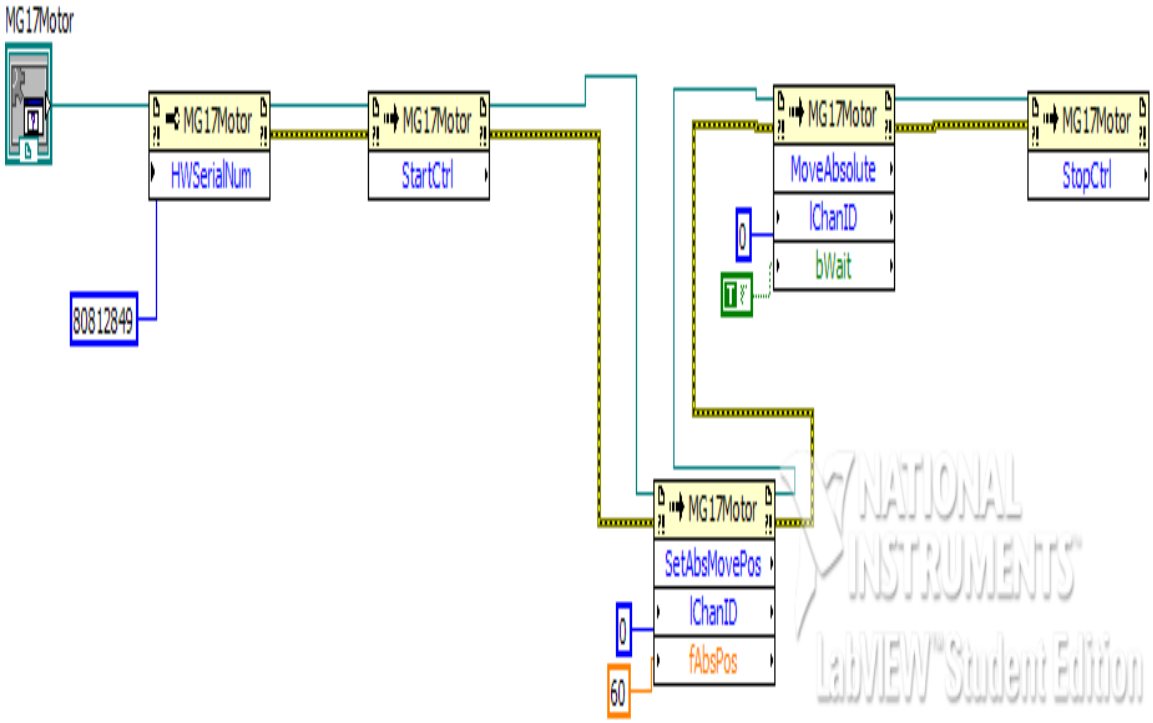

Figure 2.17 The Figure is a screenshot of the program that controls the filter wheel. The serial number of the device is read, the control is started, and the position of the filter wheel is set and moved back to its original position. The program is then stopped.

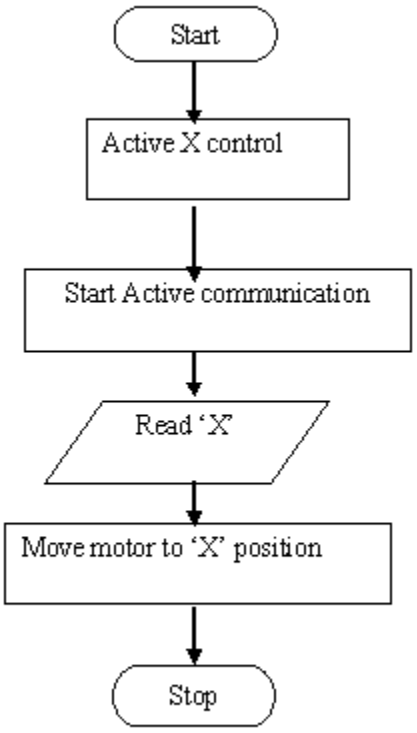

Figure 2.18 The Figure depicts the flowchart of the program that controls the filter wheel. The Active X control starts the communication, moves the position of the filter with respect to the filter wheel and stops the program

2.8.11.4 Controlling the CCD camera

The program to control the CCD camera was written in Visual studio. The executable was called using NI LabView. The program written to control the SenSys CCD camera has an option to run the camera in strobed mode. This allowed for controlling the camera using pulses.

2.8.11.5 Integrating the functions into the program

The final program has five different VIs placed together in a flat sequence structure. Different experiments could be conducted by changing the order of sequence of these

VIs. For example, in the above sequence of events, the two pulsed light sources are alternately triggered along with their respective images displayed alternately to target the two channels in the neuronal network. After a few pulses, the filter wheel is triggered to illuminate the entire field of view with 340nm wavelength light. Then the camera is triggered to acquire a picture. After this event, the filter wheel is triggered once again to illuminate the field of view with 380nm wavelength light. The camera is once again triggered to acquire a picture. The ratio of these images is considered to provide the ratiometric quantitative measure of calcium in the cells. The camera used for this purpose is the SenSys Photometrics camera to provide subtle changes in intensity during calcium imaging. The integration of the system design with biology is discussed in the following Chapter.

CHAPTER 3

SYSTEM CHARACTERIZATION

3.1 System Integration

The system is an integration of DLP optical sub-system and an epi-fluorescence inverted microscope accessorized using Light sources, Image acquisition systems and a filter wheel by Thor Labs controlled by NI LabView program. The integrated system functions as an instrument that could potentially be used for neurological studies. The system integration is discussed in the following section.

3.1.1 Integration of DLP with microscope

The optical sub-system of the instrument uses the Digital Micromirror Device (DMD) to selectively direct light to different regions on to the petri-dish containing neurons. The optical sub-system is described as follows:

Three light sources were used in this work as depicted in Figure 3.4. Two strobe lamps were used to put out blue and yellow pulses of light and a Lightning Cure UV Spot Light Source with a 200W Mercury Xenon lamp was used for Fura-2 readout. In addition, a three branch fiber light guide was installed which projects light onto the DMD via the optical pathway.

The illumination system collects the light from the HgXe lamp with the quartz fiber optic cable and relays the light to a quartz integrator. Texas instruments developed the quartz integrator rod for commercial DLP computer projection systems. The quartz integrator rod serves two purposes in the DOC system: first, the rod integrates the light intensity from the strobe lamp uniformly over a small area, and secondly the rod maps the light to the same aspect ratio as the DLP. The band of light is magnified using the magnifying lens prior to projection onto the DMD via flat front and spherical mirrors. The front surface mirror is mounted on an optical rotation mount (Newport part #RSP-2). An Opticlaw from New Focus (New Focus,

part # 9854-K) was used to hold the spherical mirror. The spherical and flat surface mirrors were adjusted using the optical rotation mount and the Opticlaw. The spherical mirror, a 50mm focal length concave mirror, focused the light onto the DMD.

The DLP sub-system of the instrument included an analog card, digital video card, video receiver and a Digital Micromirror Device (DMD) [57]. The analog video and digital video driver cards interface with the computer through a PCI slot. The monitor of the computer transmits the image of the digital pattern to the video receiver card of the DLP sub-system. The video receiver card then sends the image of the pattern to the DMD which is then projected onto the collecting lens. The image pattern is created in Microsoft Paint and transmitted to the DMD as a .bmp file.

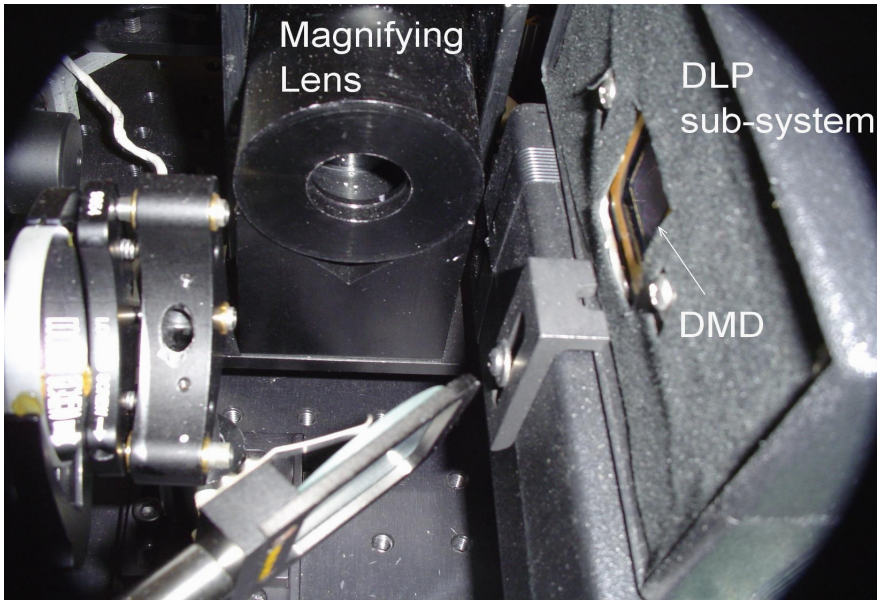

Figure 3.1 The figure shows the optical sub-system with DLP sub-system and magnifying lens. The integrator rod and magnifying lens convert the light from the fiber optic cable to the same aspect ratio as the DMD

Figure 3.1 shows the position of the magnifying lens, DMD and the mirrors. The magnifying lens and the mirrors direct the light towards the DMD. The DMD projects the patterned light towards the collecting lens that focuses the patterned light onto the petri-dish.

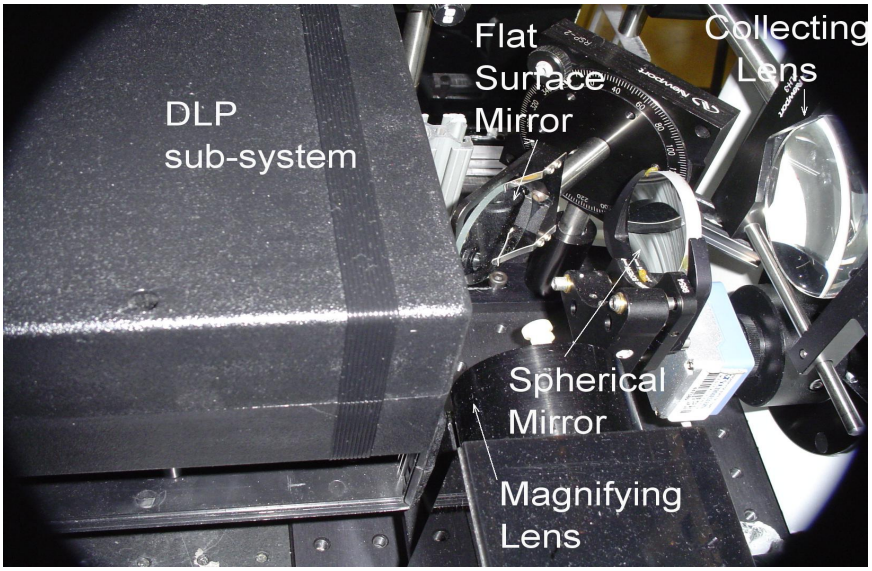

Figure 3.2 The Light from the fiber optic cable is projected onto the flat surface mirror via the integrator rod and the magnifying lens. The light is then directed towards the spherical surface mirror that directs the light towards the DMD. The DMD projects the patterned light towards the collecting lens

The figure 3.2 shows the optical sub-system. The light travels from the integrator rod and magnifying lens towards the mirrors that direct it towards the DMD. The DMD modulates this light with the gray scale pattern on the DMD and projects the resultant patterned light towards the collecting lens. Also visible in the picture are the mirror holders that can be tuned to direct the light path appropriately.

3.2 System Operation

The system is run in two stages for controlling and manipulation of neural circuits. The final design of the system is discussed herein.

3.2.1 Generating Digital light masks for spatial selectivity of neurons/neural components

To target a structure on the system, it is important to initially find the spatial location of the selected structure and convert the acquired spatial location into a pattern that can be displayed on the DMD.

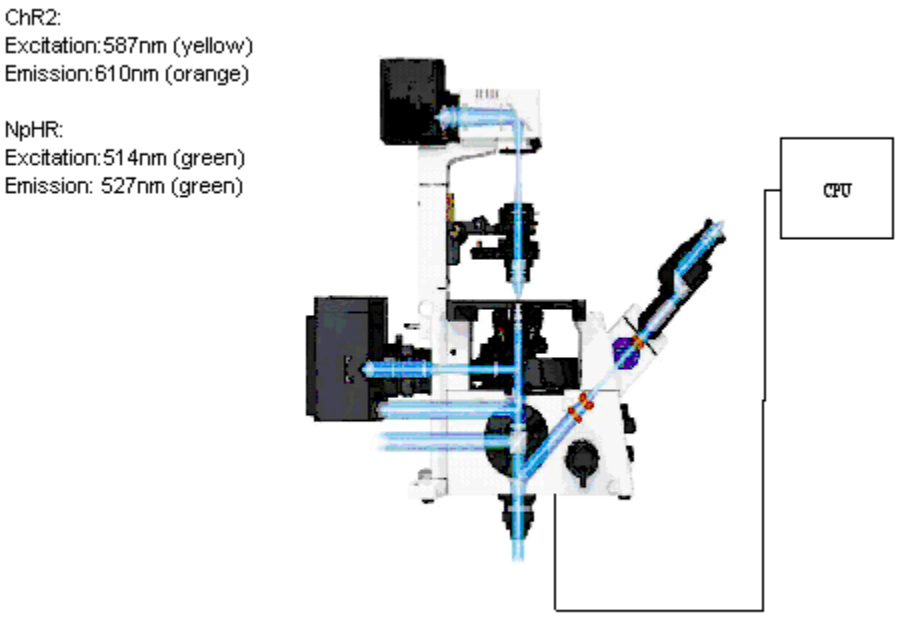

Figure 3.3 The figure shows the wavelengths at which the two channels-ChR2 and NpHR are visible. The pictures of their locations are acquired and converted to gray scale images depending on the channels selected to be targeted.

As shown in figure 3.3, the filter turret is initially positioned to view the ChR2 channels through the mCherry filter cube. The mercury lamp that is fixed on a port on the microscope is switched on and allowed to stabilize. The shutter in front of the lamp is opened and the light is then allowed to project onto the filter cube. The filter cube reflects between approximately 530nm to 580nm with approx 95% transmission at 560nm. This light triggers mCherry fluorescence and allows us to determine the spatial location of ChR2 channels. Images are acquired using the Motic camera. The number of pixels on the pattern is equivalent to the number of mirrors (=pixels) on the DMD and hence the digital mask created coincides with the spatial location of the target cells/cellular components (pixels of the pattern adjusted in IDL). The digital mask is determined based on the neurons to be targeted or the sub-cellular components of the neurons to be targeted. A digital mask is a gray scale image. It can be used

to project different intensities on different cells or different parts of the cells. In this case, we use a binary digital mask. This mask will be used to illuminate either cells or cellular components with light. This procedure is then repeated for finding the spatial location of the NpHR channels. However, we use an EYFP filter cube since the NpHR channels are tagged to EYFP fluorescent dye. The filter cube reflects between 490nm to 510nm with approximately 95% transmission at 500nm. This light triggers EYFP fluorescence and allows us to determine the spatial location of NpHR channels. Images are acquired using the Motic camera. Digital masks can then be created and NpHR channels thus targeted. In conclusion, we thus generate two image patterns: one for targeting ChR2 channels and the other for targeting NpHR channels. This allows for depolarizing and hyperpolarizing the cells respectively.

3.2.2 Control/Manipulation of neural circuits

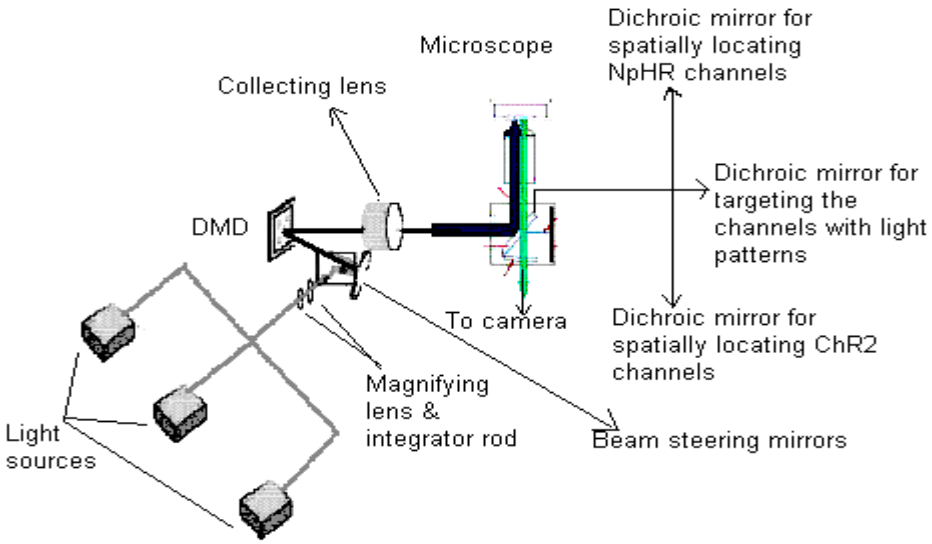

Figure 3.4 The final design setup is shown in the above picture. The three sources of light are integrated into the system using a fiber-optic cable.

Figure 3.4 depicts the system setup. The UV lamp and strobe lamps are switched on and allowed to stabilize for 15 minutes. The NI LabVIEW program is then run. The program initializes the pulsing of the strobe lamp. The digital mask corresponding to the target ChR2 channels is sent to the DMD via the video card. The pulsing is allowed to continue for a pre-determined time. The program then overlaps the yellow wavelength pulses by switching off the blue wavelength strobe lamp and initializing the yellow wavelength strobe lamp. In this case, the digital mask corresponding to the spatial location of the target NpHR channels is sent to the DMD via the video card. The pulsing is allowed to continue for a pre-determined time. At the end of these pulses, the filter wheel is triggered in order to position the 340nm filter in front of the UV lamp and a digital mask corresponding to the full illumination of the field of view is sent to the DMD via the video card. At this point, an image is acquired which corresponds to the Fura-2 imaging at 340nm. After a short fraction of a second (ideally to be immediately after the first image acquisition but limited by the hardware characteristics), the filter wheel is triggered in order to position the 380nm filter in front of the UV lamp. The digital mask corresponding to the full illumination of the field of view is allowed to stay on the DMD. At this point, an image is acquired that corresponds to the Fura-2 imaging at 380nm. The ratio of the two images gives the intensity based calcium concentration “spots”. These “spots” can be characterized as hot spots and cold spots. The hot spots and cold spots would correspond to the spatial locations of maximum and minimum calcium concentration intensities respectively. Table 3.1 gives an overview of the wavelengths of light required to determine the spatial locations of the channels and also the wavelengths of light required to trigger them.

Table 3.1 The table depicts the wavelengths of light required to view the channels and trigger them.

Channels	Wavelength for viewing the channels (nm)	Wavelength for triggering the channels (nm)
ChR2	Approx 560	Approx 470
NpHR	Approx 500	Approx 580

3.3 System parameter

3.3.1 Converting pixel size to feature size on the petri-dish

The optical setup is such that the light collecting lens is at a distance of 16cm from the DMD and 16.6 cm from the base of the objective on the microscope. Hence there is a magnification factor of 1.0375 due to the lens. If the objective used has a magnification factor of 10, the total magnification due to these lenses would be 10.375.

According to the technical specifications of the DMD, each mirror is a 17µm x17µm in size including the spacing between them. This mirror on the DMD corresponds to one pixel. Hence each pixel corresponds to 1.639µm on the slide (considering the magnification due to the lenses). Thus, a 1024 x 768 pixel matrix on the DMD converts to a 1678µm x 1258µm image on the slide.

3.3.2 Determination of the Switching time of the DMD and the switching time between two patterns

The DMD switching time is the time required to change the state of a mirror from ON to OFF or vice versa. This switching time is given as 21µsec [58]. The switching time between two patterns is on the order of milliseconds because the system is operated using NI LabView. It is depicted in Figure 4.25 in Chapter 4.

CHAPTER 4

RESULTS AND DISCUSSION

4.1 Demonstration of spatial resolution of the system on a glass slide

The spatial resolution of the system was initially demonstrated on a glass slide with different sized “dots”. The dots that were tested included 1.5mm, 0.6mm, 0.15mm and 0.07mm. This slide was placed on the microscope such that the pattern was projected either overlapping the dot or beside the dot. The following figures from Figure a) to 0) depict the different patterns projected through the DMD onto the specimen. The patterns were provided by Lynntech, Inc in .JPEG format.

4.1.1 System setup

The system setup remained the same as described in Chapter 2 except for the light source, the fiber optic cable coupling the light source with the optical sub-system and the filter cube in the microscope. The fiber optic cable used in this case is a UV transmittance cable from Oriel as described in Chapter 2. The UV light source was used to project a UV pattern on the specimen. It can be noted here that any other wavelength of light could be used for the projection with a matching set of optics. UV light was used only for convenience and ease of availability of filter sets at the time of conducting the experiments. The following figures depict the spatial resolution of the system with the system setup briefed above.

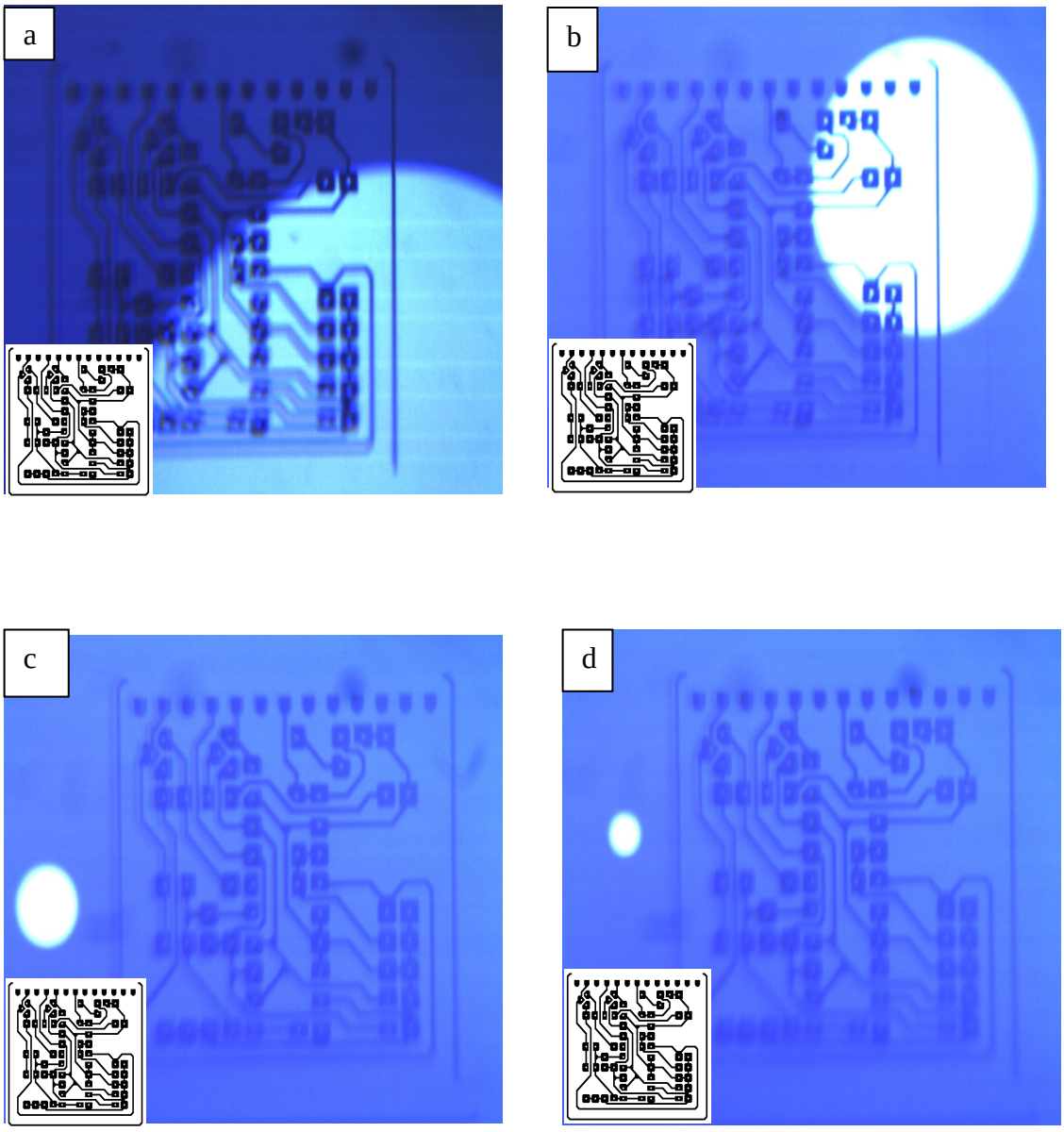

Figure 4.1 The Figures from a) to d) depict the spatial resolution of the system using a ‘circuit board pattern’ projected from the DMD onto a microscope slide with different sized ‘dots’

In the Figures from a) to d), the pictures in the inset are the .bmp files that were displayed on the DMD using video cards. The inset pictures from Figures a) to d) depict a 'Printed circuit board' pattern which is modulated with UV light and focused through the dichroic mirror of the microscope via a lens. The inset picture in Figure a) was focused onto the 1.5mm dot on the glass slide placed at the tip of the objective. In the same way, in Figures b), c) and d), the inset pictures were focused on to the 0.6mm dot, 0.15mm dot and 0.07mm dot on the glass slide respectively. Motic camera was used to acquire these pictures. The U-MWU filter set was used on the microscope. It emission filter allows all wavelengths above 420nm to pass through them. Since the UV light source puts out some part of the blue wavelength of light, it was possible for the Motic camera to acquire the above pictures.

4.1.2 Discussion

The above Figures depict the range of binary pictures that could be well focused onto the specimen at the objective tip and prove that the spatial resolution of this system is high enough to selectively target cells or sub-cellular organelles of cells in a given petri-dish of cells. These pictures also high light the capability of the system for 'spatial selectivity' which could be used for biological applications to target cells that respond to different wavelengths of light. The spatial resolution of the system was calculated to be 0.448 microns (by Amruta Joshi in her thesis work). It has already been shown that fibroblast cells could be studied on this system by selectively targeting different parts of the cells and by selectively targeting the cells of interest in a given field of view of the system. More information regarding this could be obtained in reference [56].

4.2 Observation of Single Neuron and Neuronal network

Fluorescent dyes could be employed to view neurons. Various dyes bind to different regions of these neurons. In the following figures, neurons tagged to GFP (Green Fluorescent Protein) and DAPI (4',6-diamidino-2-phenylindole) are demonstrated.

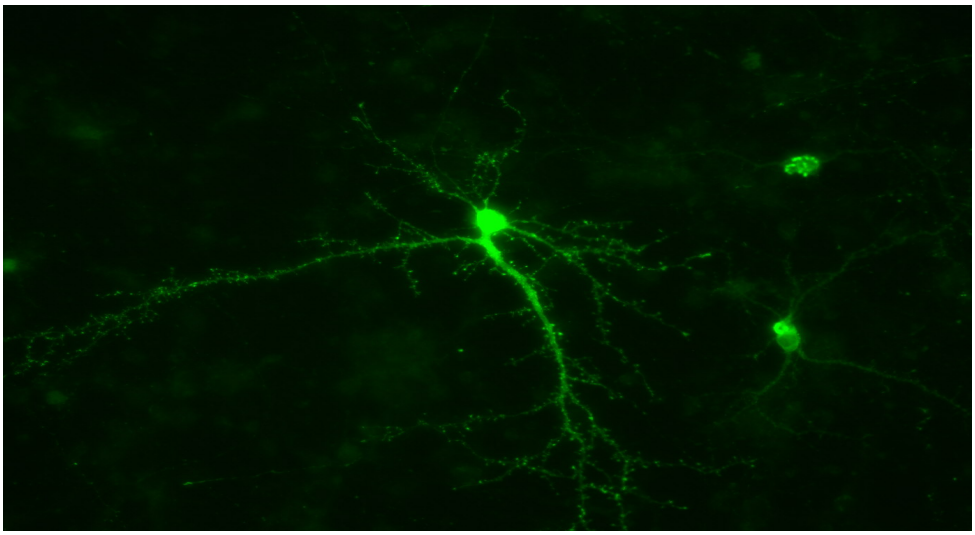

Figure 4.2 Single neuron under the influence of GFP in a field of view allows targeting sub-cellular components of the neurons. An example of sub-cellular organelles of neurons and the neural network that could be manipulated/ controlled (Courtesy: Herz lab)

GFP binds to the cytoskeleton and hence the entire neuron is clearly visible when viewed on a fluorescence microscope (20X) under a GFP filter set. Also clearly visible in the above figure are soma, axon and dendrites.

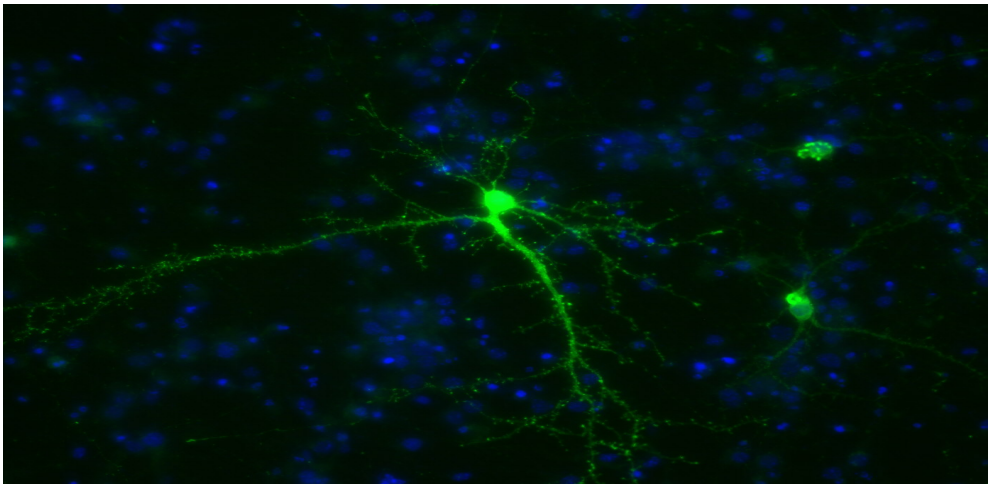

Figure 4.3 Single neuron under the influence of GFP and nuclei from other neurons stained with DAPI. An example of sub-cellular organelles of neurons and the neural network that could be manipulated/ controlled (Courtesy: Herz lab)

DAPI binds to the DNA and hence the nucleus is clearly visible when viewed on a fluorescence microscope (20X) under a GFP+DAPI filter set.

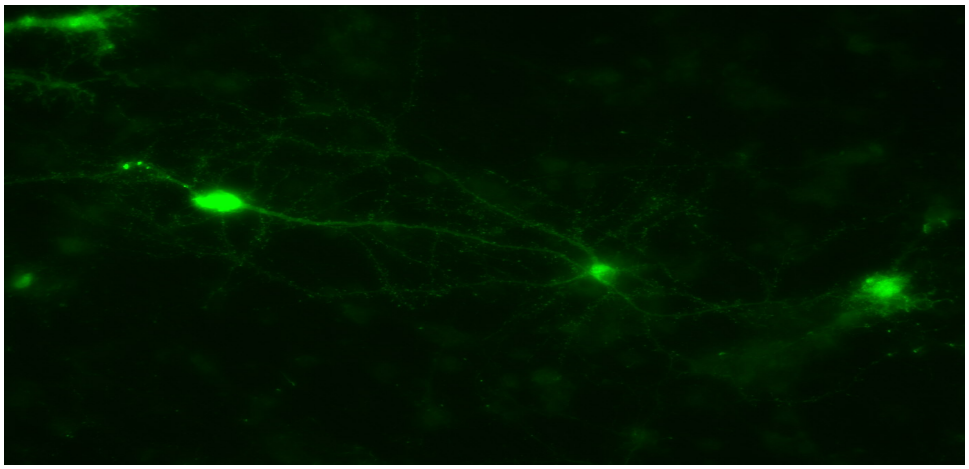

Figure 4.4 Neural network under the influence of GFP at 20X magnification (Courtesy: Herz lab)

In the Figure 4.4, the interconnections of neurons are clearly visible. Such a field of view could possibly be useful to study the interconnections of neurons once they are engineered to respond to light.

Figures 4.2, 4.3, 4.4 were captured using Motic camera. However, for higher resolution, SenSys Photometrics CCD camera was employed which has a 12- bit dynamic range. This camera can provide 4096 gray levels and hence provides an advantage when viewing subtle changes in calcium imaging readout.

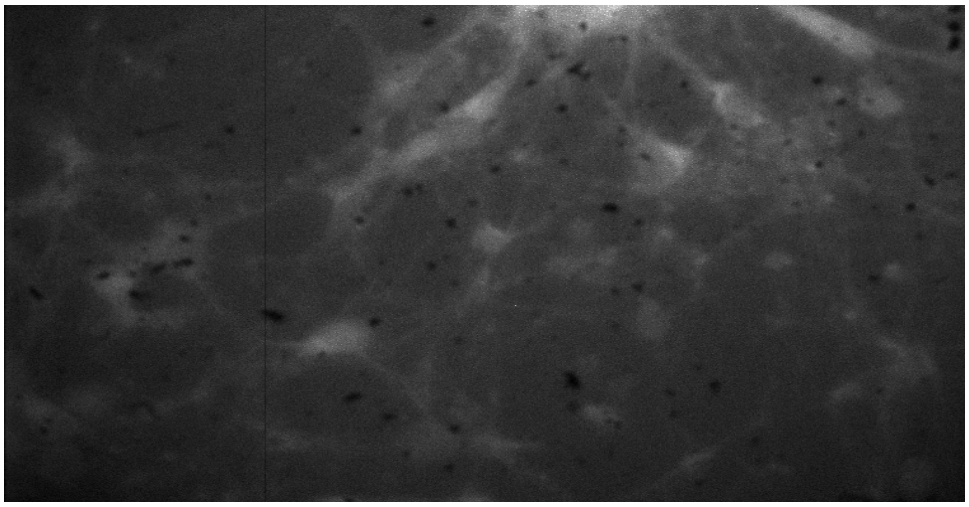

Figure 4.5 Darkfield picture of neurons viewed through a GFP filter using SenSys CCD camera. The neurons depicted in the four figures above are simply tagged with the fluorescent dyes. These neurons were to be made responsive to light to study the neural network and observe the trends in memory and communication.

4.3 Preliminary results from genetically expressing channels in neurons

As mentioned in Section 4.2, the neurons could be imaged using fluorescent dyes and manipulated once they are engineered to respond to light. Many attempts have been made by the Herz lab (UTSW) to genetically engineer neurons to respond to light. Two channels were expressed in the neurons which could depolarize and hyperpolarize the cells. These channels are called ChR2 and NpHR channels respectively. It was attempted to tag them to mCherry and EYFP fluorescent dyes, respectively, in the various experiments conducted that are described below.

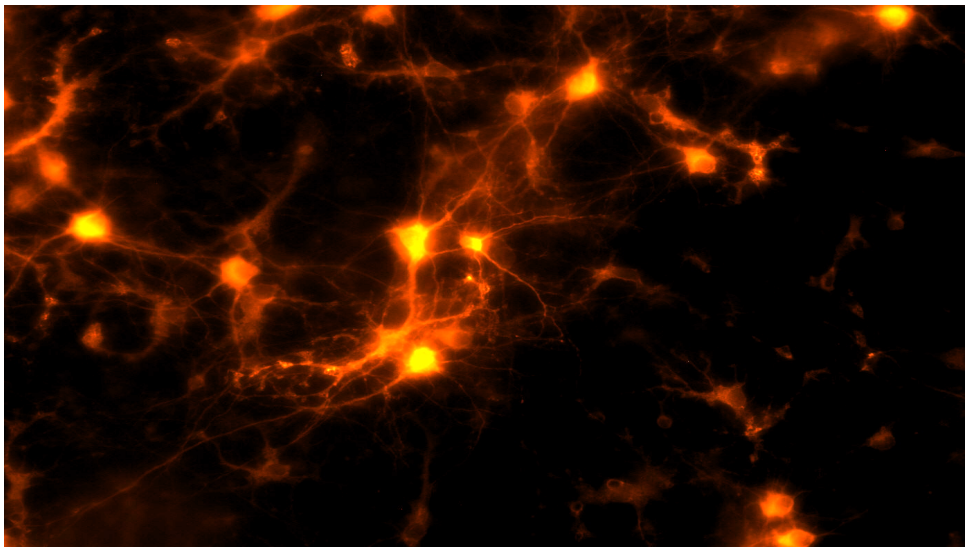

Figure 4.6 The above figure depicts primary neurons (mice) expressed with ChR2 channels and tagged to mCherry. They were observed on a fluorescent microscope (20X) under an mCherry filter set. Promoter: H64. (Courtesy: Herz lab)

The promoter used in this case was H64. The plasmid used to express the channel in the neurons was directly obtained from Deissoroth lab (Stanford University).Its size is 10.9Kb and consisted of an Ampicillin resistant gene.

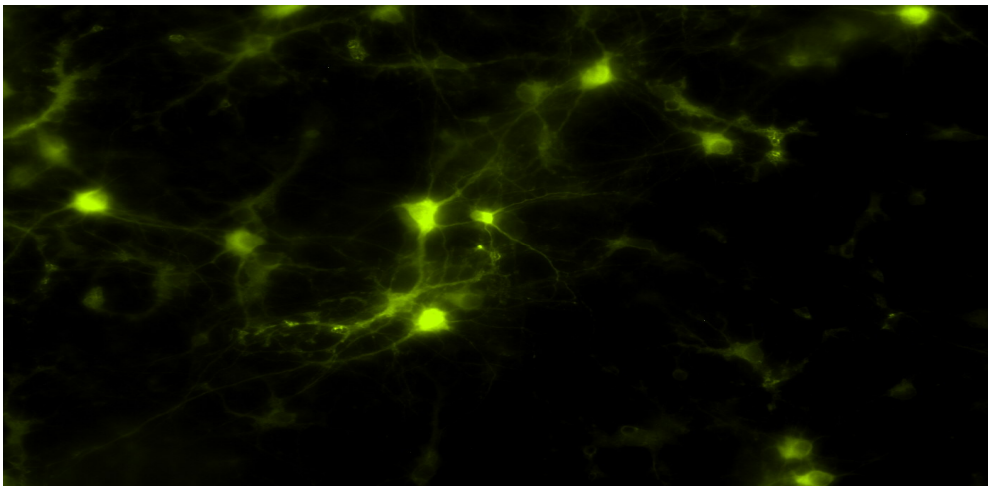

Figure 4.7 The figure depicts primary neurons (from mice) with NpHR channels genetically expressed in them. They were observed on a fluorescence microscope (20 X) under an EYFP filter set. Promoter: H64 (Courtesy: Herz lab)

This work was initially accomplished at Stanford University by Deissoroth lab and the plasmids were sold to Herz lab (UTSW). The genetic expression of the primary neurons was carried out in the Herz lab (UTSW). The promoter used to express the NpHR channels was H64 with a size of 10.9Kb and had an ampicillin resistant gene on it.

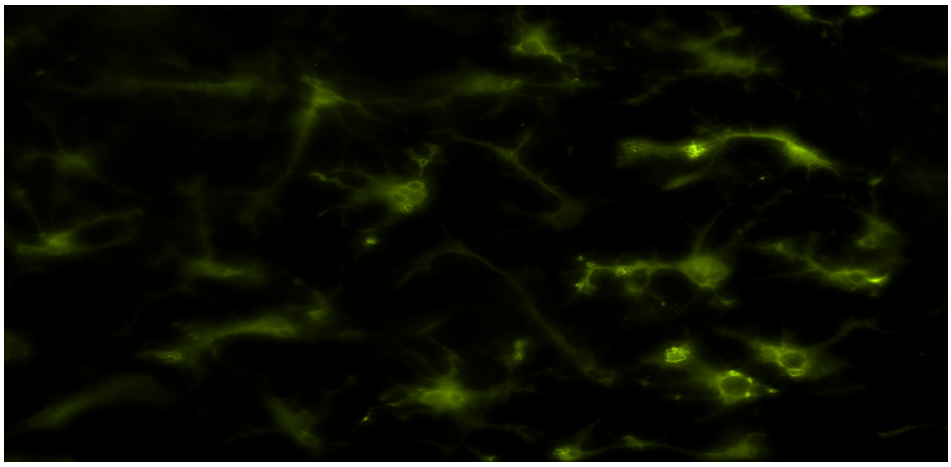

Figure 4.8 The figure depicts primary neurons (from mice) with NpHR channels genetically expressed in them. The promoter used to express the NpHR channels was NSE (neuronal-specific enolase). (Courtesy: Herz lab)

The viewing of the channels was achieved on a fluorescence microscope (40X) under an EYFP filter set. The objective in using this promoter was to express the channels exclusively in the hippocampal neurons.

The difference between Figures 4.5 and 4.6 can be clearly observed. The level of expression of the channels in the neurons is lower in Figure 4.6 when compared to Figure 4.5. This could be attributed to the change in promoter in the neurons depicted in Figure 4.6.

Expressing neurons with ChR2 channels tagged to mCherry (Promoter NSE), however, did not yield any visible fluorescence. This might be attributed to the low rate of expression when the NSE promoter is used. Also, testing depolarization before hyperpolarization is extremely important. Hence, to prepare neurons with visible ChR2 channels is very essential to proceed with the experiments. Thenceforth, all experiments will exclusively consist of neurons that have been expressed with ChR2 channels and tagged to EYFP.

4.4 SenSys and Motic cameras

Keeping the field of view approximately constant, it is interesting to observe the neurons under different imaging conditions as depicted in the following figures.

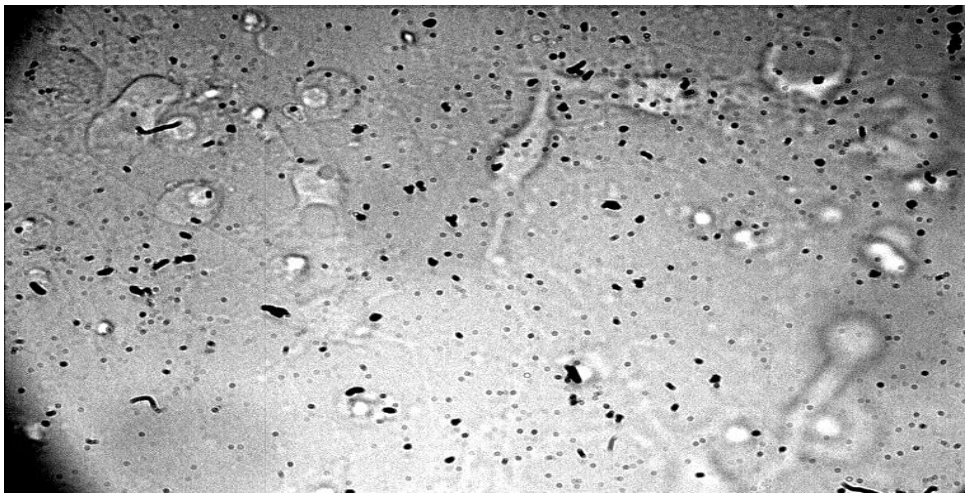

Figure 4.9 Brightfield picture of neurons under the influence of GFP at 60X using SenSys camera

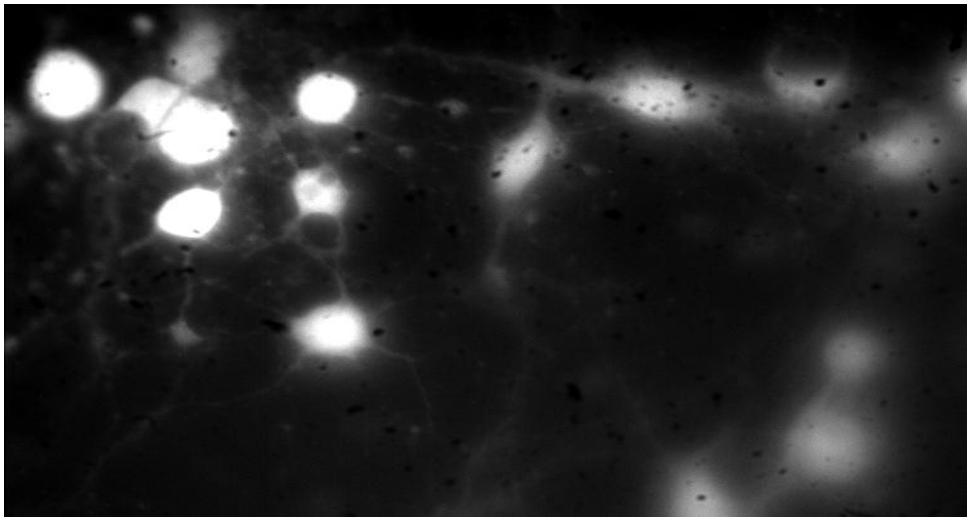

Figure 4.10 Darkfield picture of neurons under the influence of GFP at 60X using SenSys camera

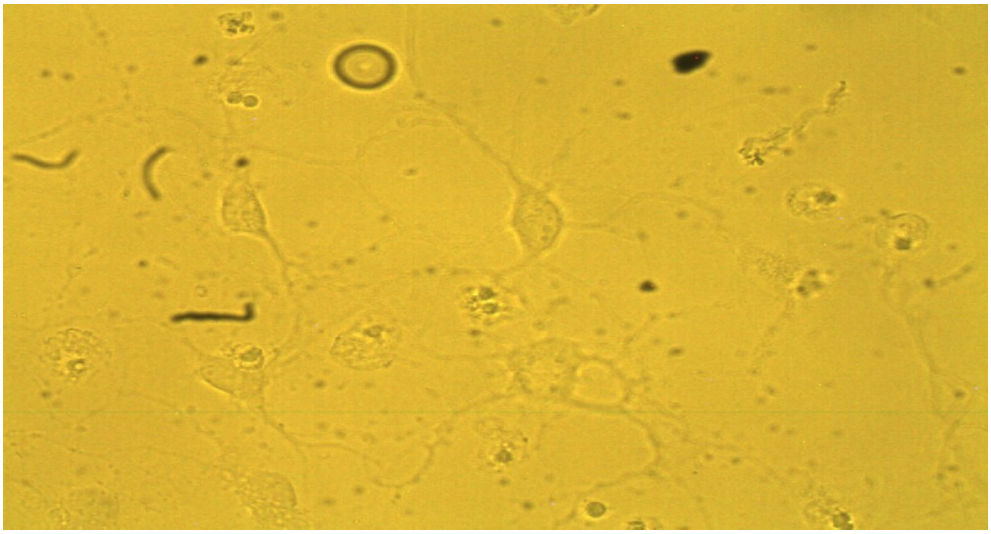

Figure 4.11 Brightfield picture of neurons under the influence of GFP at 60X using Motic camera

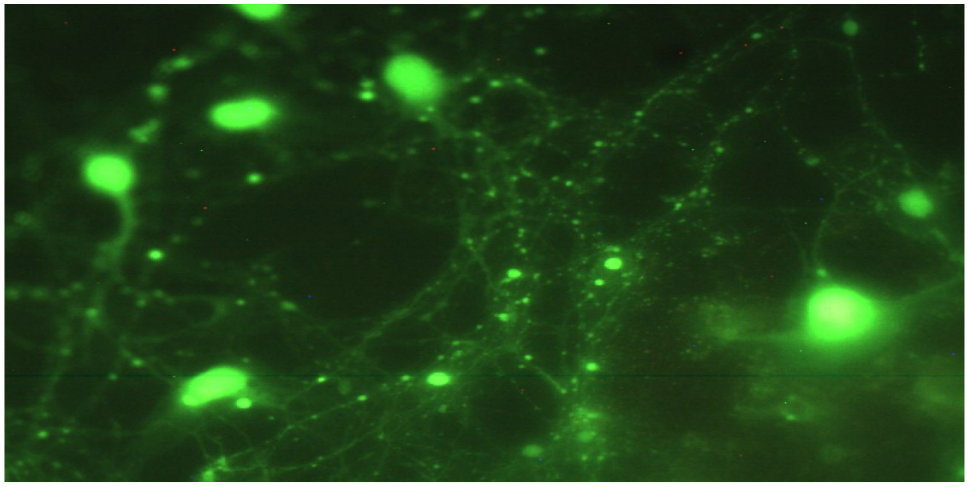

Figure 4.12 Darkfield picture of neurons under the influence of GFP at 60X using Motic camera

From the above pictures, it is clear that both Motic and SenSys camera can detect the fluorescent labeled neurons. However, the pseudo-coloring in the Motic camera is more prominent when compared to the SenSys camera. Hence it is used in identifying the locations of the channels and for generating patterns. The calcium read-out will still be imaged using SenSys camera because of the fact that SenSys camera is capable of detecting subtle changes in intensities and also has faster shutter speeds than Motic camera. Also worth mentioning is

the fact that the pictures taken with these cameras are corrected to 1024x 768 pixels (to match the DMD pixels) by using an IDL (Interface Descriptive Language) program written by Michael Huebschman.

4.5 Photobleaching

Photobleaching was confirmed with this experiment. Trolox was used as an anti-oxidant to reduce the oxidative stress and reduce the photobleaching for a few minutes.

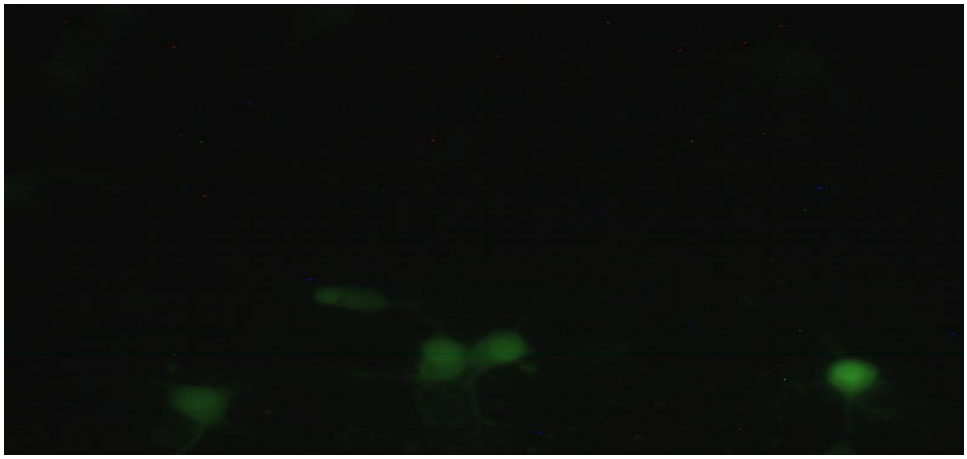

Figure 4.13 Neurons expressed with ChR2 channels and tagged to EYFP. This figure depicts the neurons the instant after exposing them to green light.

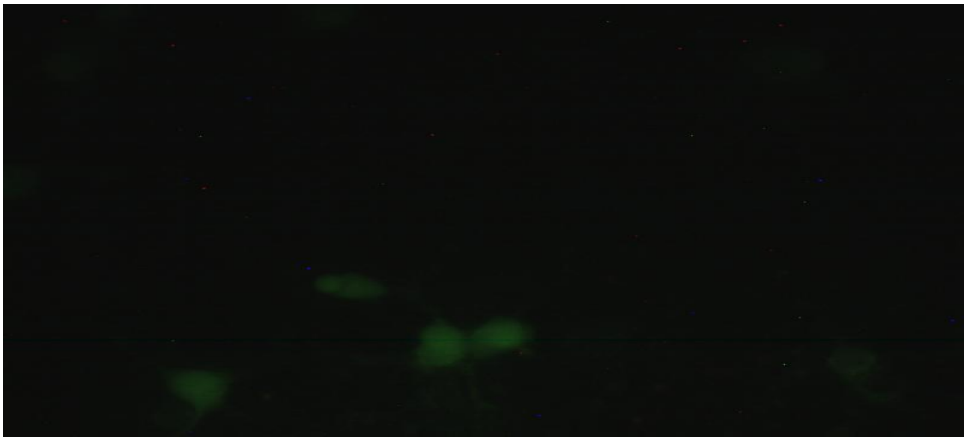

Figure 4.14 Neurons expressed with ChR2 channels and tagged to EYFP. This figure depicts the neurons after 39 seconds of exposing them to green light. Photobleaching is confirmed.

From the Figures 4.13 and Figure 4.14, it is evident that the fluorescent dye EYFP photobleached after sometime. The photos were taken by the Motic camera at the same settings without digital alteration for this visual comparison. The time taken for this photobleaching was 39 seconds. The Motic camera recorded the pictures at the rate of 10fps. Hence, at the rate of one frame every 100ms, 390 frames were captured. However, Image J software was used to analyze the frames and the software reduced the 39 frames into 101 frames. The figures 4.13 and 4.14 were obtained after opening the file in Image J.

4.6 Testing the presence of ChR2 channels

Testing for the presence of channels was performed in three ways.

1) Using electrophysiology 2) Using Drug Trigger and 3) Using Light Trigger

4.6.1 Using Electrophysiology:

Initially, the traditional electrophysiology technique was used to test for the presence of ChR2 channels. The following graph is the result of this technique.

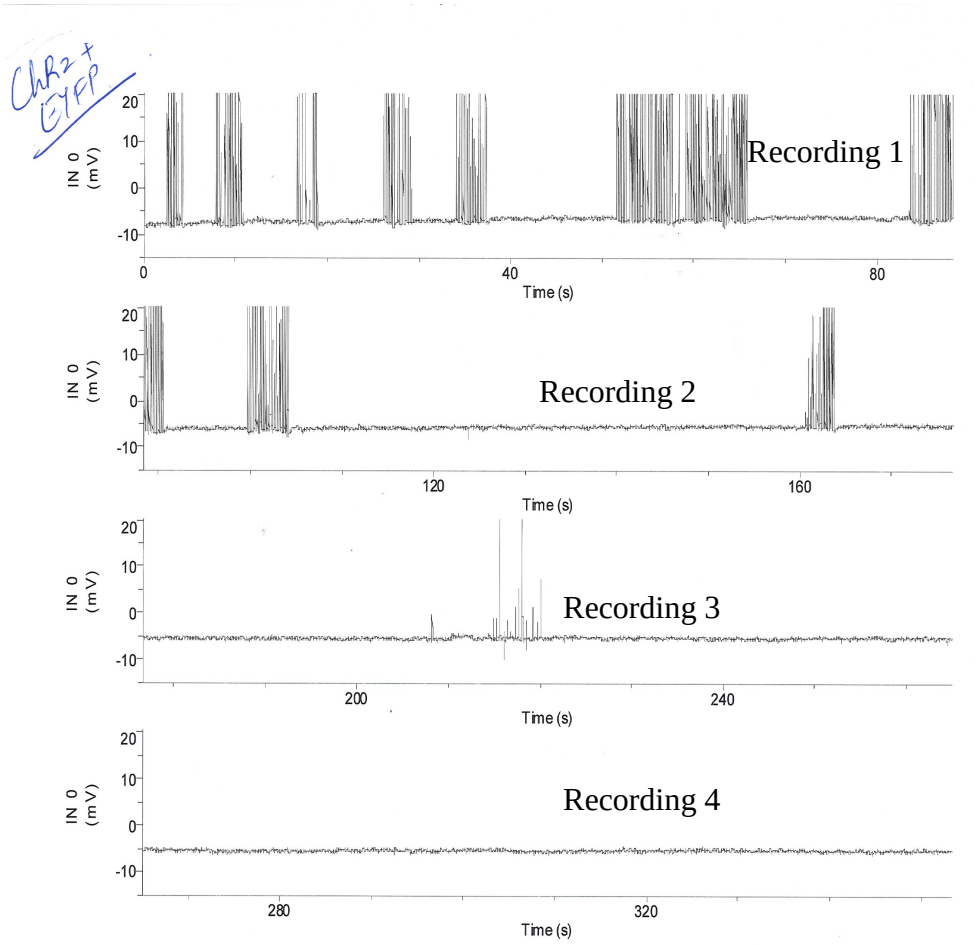

Figure 4.15 Electrophysiology testing for the presence of channels (Courtesy: Herz lab)

In the Figure 4.15, the neuronal cells were tested for the presence of ChR2 channels. The experimental setup, observation and conclusions are as described below.

A) Experimental setup: Patch clamping technique was used to test for the presence of channels. Pulsed blue light was used to shine on the entire petri-dish of cells. One electrode was used to measure the voltage spike in a specific neuron.

B) Observation: It could be observed in recordings 1, 2 and 3 that in the presence of light pulses, the electrode measured some voltage represented in the form of voltage spikes. Also, in recording 3 it could be observed that decreasing the frequency of pulses of light decreased the frequency of voltage spikes. In recording 4, light pulses were absent and correspondingly, no

voltage spikes were observed.

C) Conclusion: The increase in voltage spikes in the presence of light and the change in the frequency of the former with respect to the later confirm the presence of a light responsive component in these cells. Since in this case, the cells were manipulated to express ChR2 channels, the presence of these channels can be confirmed.

4.6.2 Using Drug Trigger

Glutamate was used as a triggering agent to prove the presence of channels and that fluo-3 fluorescent dye was responding accordingly. The following Figures 4.16 and 4.17 were analyzed using ImageJ. Neutral density filter was used to reduce the intensity of the Hg lamp which reduced the rate of photobleaching to a certain extent.

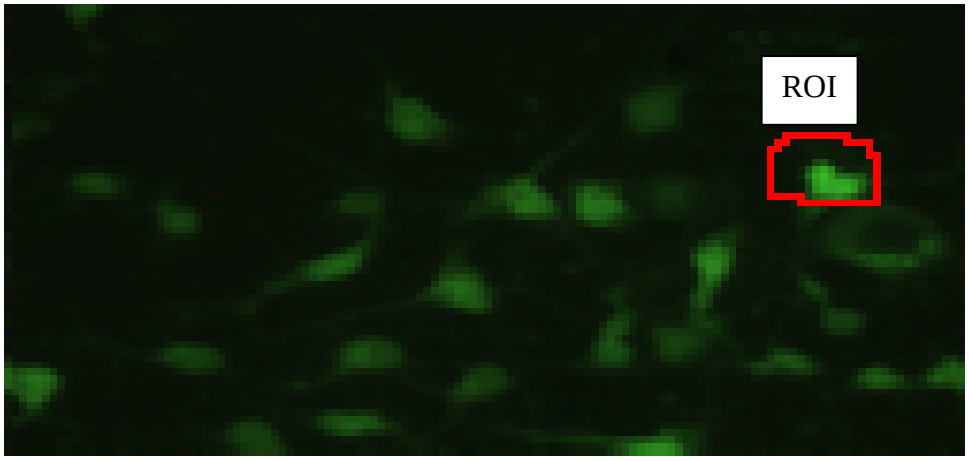

Figure 4.16 The figure depicts neurons with fluo-3 at the next instant of trigger (glutamate trigger). ROI indicates the Region of Interest where a change in intensity was observed

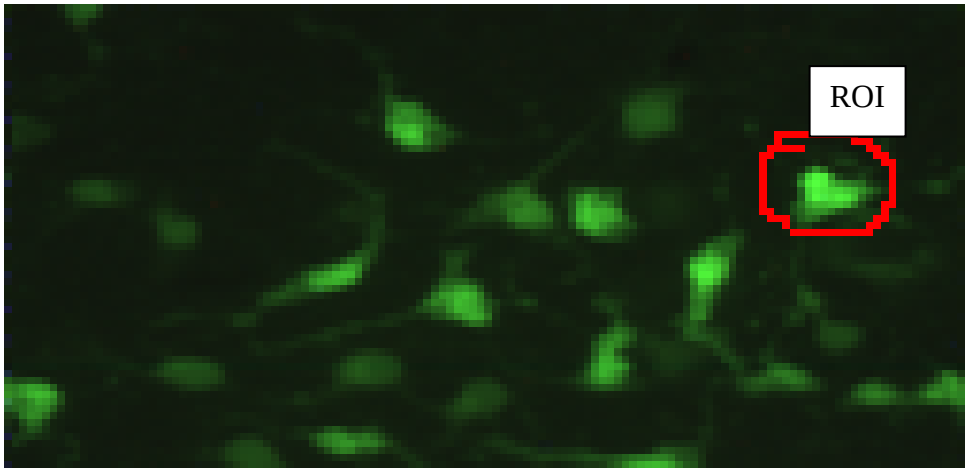

Figure 4.17 The Figure depicts neurons with fluo-3; 104th frame after trigger (glutamate trigger). ROI indicates the Region of Interest where a change in intensity was observed.

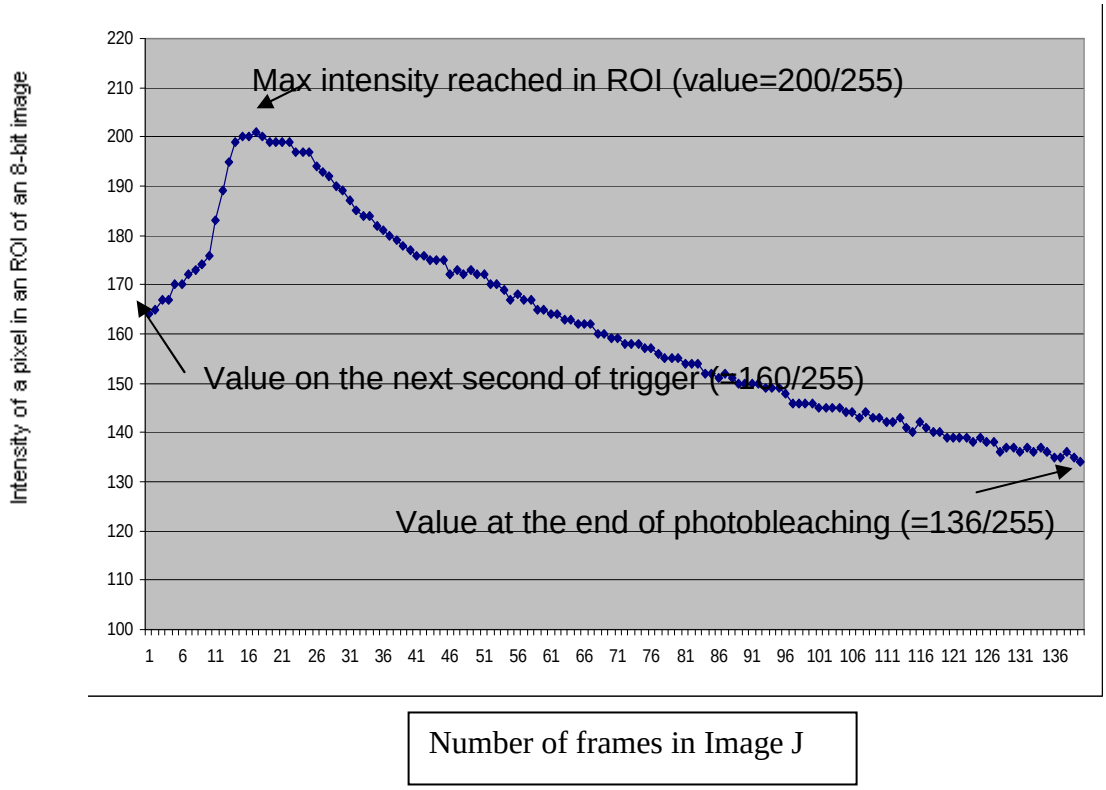

Figure 4.18 Dynamic intensity values vs. number of frames in Image J resulting from glutamate triggering of neurons.

The figures 4.16 and 4.17 depict a positive control for the presence of fluo-3.

This experiment was necessary as one of the fluorophores used; EYFP has the same spectral characteristics as that of fluo-3.

A) Experimental setup: The neuronal cells were loaded with 0.5microliters of fluo-3. ACSF was added to the petri-dish after a few hours, to increase the concentration of extracellular calcium. Glutamate (50 microliters) was added to the dish of cells just before beginning the experiment. The picture was taken every 100ms using Motic camera. The intensity plot was made by selecting a pixel in the ROI and manually noting down the intensity values of the green color for each frame.

B) Observation: There was an increase in the intensity of fluorescence of fluo-3 as shown in the Figure 4.25. However, after the intensity reached a certain value, it began to decrease.

C) Conclusion: The increase in fluorescence intensity of fluo-3 can only result from its binding to calcium. The decrease in intensity after a certain value could be due to photobleaching as the filters used in this case are ET sputtered filters from Chroma technologies that allow a large amount of excitation light to hit the petri-dish. Also, fluo-3 has a fast bleaching rate. Thus the presence of fluo-3 could be tested for.

4.6.3 Using Light Trigger

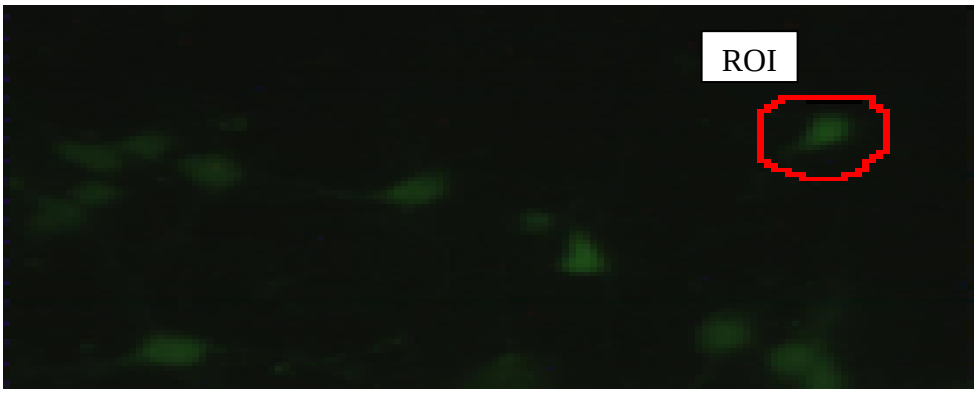

Figure 4.19 The figure depicts neurons with fluo-3 at the next instant of trigger (light trigger). ROI indicates the Region of Interest where a change in intensity was observed

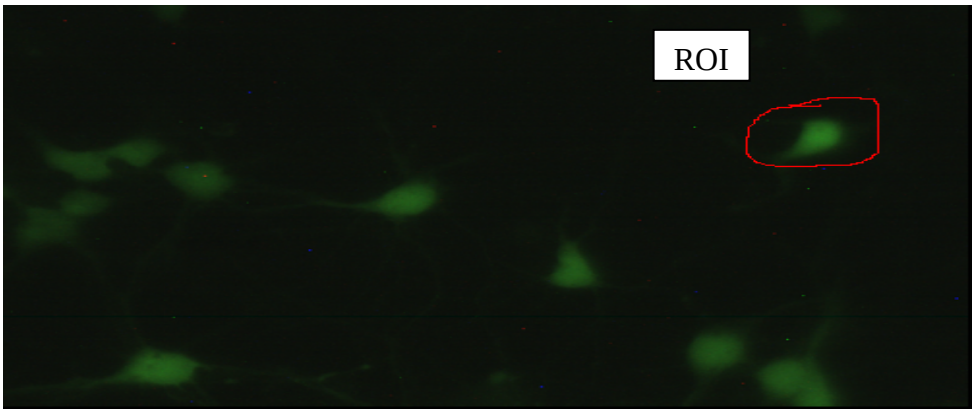

Figure 4.20 The Figure depicts neurons with fluo-3; 104 frames after trigger (light trigger). ROI indicates the Region of Interest where a change in intensity was observed.

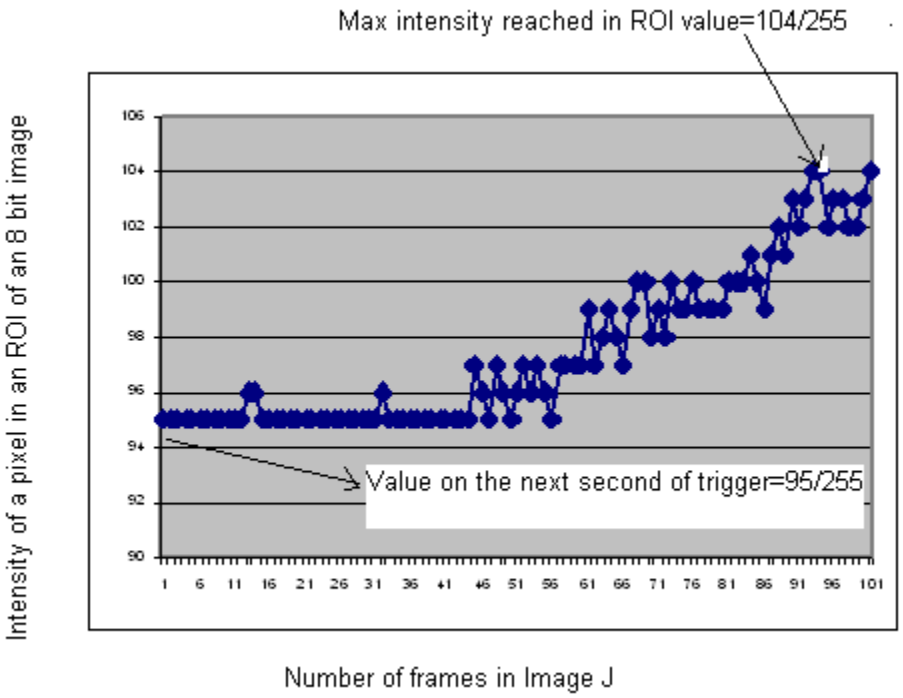

Figure 4.21 Dynamic intensity values vs. number of frames resulting from light triggering of neurons

This experiment deals with testing for the presence of ChR2 channels using the fluo-3 fluorophore.

Experimental setup: The neuronal cells were loaded with 0.5microliters of fluo-3.After a few hours; ACSF was added to the petri-dish to increase the concentration of extracellular calcium. The entire field of view (unlike the entire petri-dish in the earlier case) was illuminated with blue light from a mercury lamp.

Observation: The fluorescence intensity of fluo-3 increased with time but the intensity rise was visibly low.

Conclusion: The increase in fluorescence intensity can be accounted for the fluo-3 binding with calcium. The calcium influx can occur only when the channels allow calcium to flow into the cell in this case. Hence we can conclude that the channels responded to light by allowing calcium to flow through them.

4.7 Using DMD for spatial selectivity of neurons

To target neurons, it is essential to initially locate the neurons with channels and then create a pattern to be projected through the DMD. In the following sections, a simple pattern will be projected onto the specimen and then a description of the attempt to view the channels will be discussed.

4.7.1 Demonstration of spatial patterning of neurons

The novelty in this system is the spatial selectivity of the neurons. Also, the spatial resolution of the system permits targeting the sub-cellular organelles in the neurons. The Figure 4.18 describes the spatial selectivity of the system. A “plus” sign with neurons in the background can be observed.

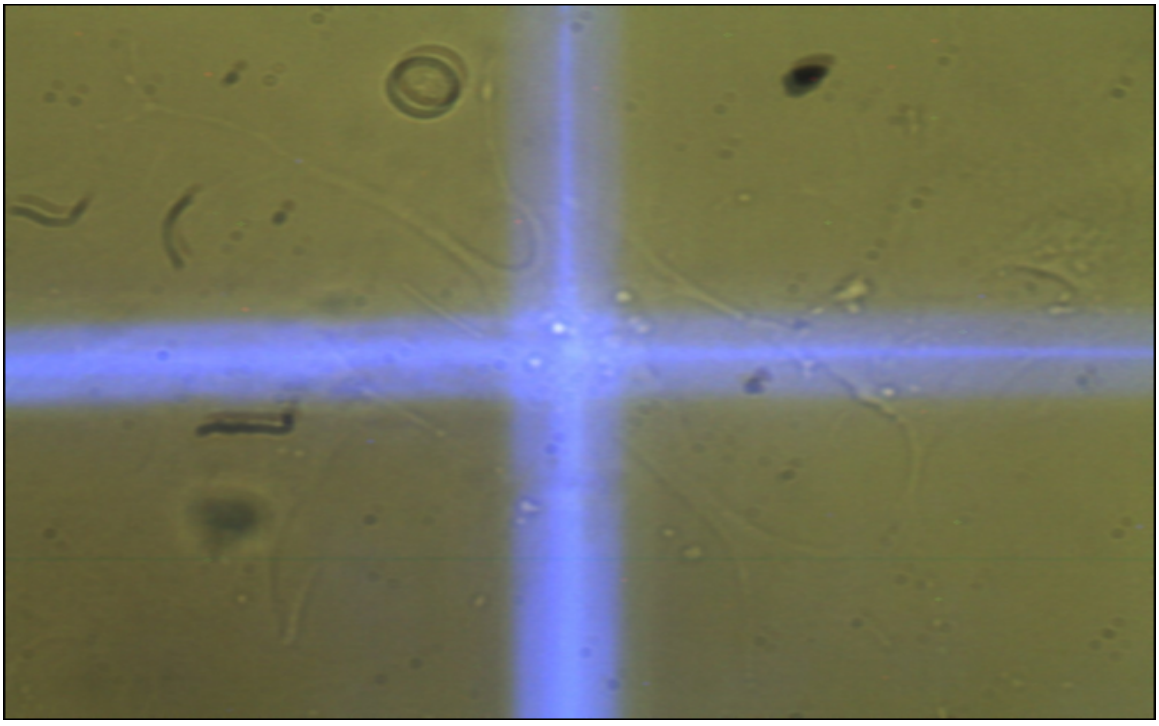

Figure 4.22 Blue light from the fiber optic cable modulated with a “plus sign” pattern on the DMD projected onto a Petri-dish of neurons viewed through a dry air 60X objective on an inverted microscope.

To be observed in the above figure is a thin line of “plus sign” surrounded by an “aura” of thick line “plus sign”. This was a pattern created on the DMD to demonstrate that not only does the DMD project binary patterns but also patterns that have different shades of gray. The brightest shade of gray (value=255 of an 8-bit image) was used for the center portion of the “plus sign”.

4.7.2 Test to view the channels through the patterns on the DMD

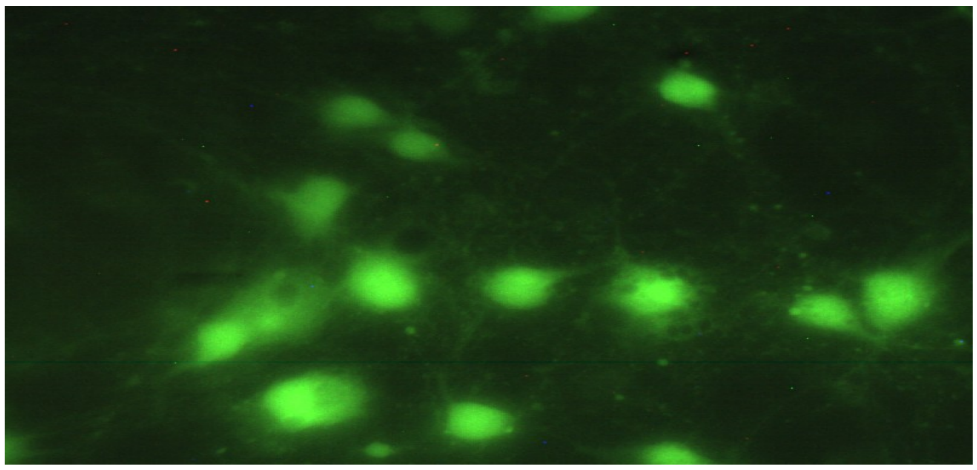

Figure 4.23 ChR2 channels expressed in primary neurons and tagged to EYFP illuminated using a Hg lamp (at 40X)

In Figure 4.23, ChR2 channels are clearly visible when illuminated with a Hg lamp and viewed using an EYFP filter set. However, no fluorescence was observed when the all the mirrors on the DMD were turned on. The intensity of light was not sufficient to excite the neurons into fluorescing. This was confirmed by conducting another test. The fiber optic cable that delivered light to the DMD was placed directly over the dichroic mirror in the microscope. The resulting is the Figure 4.24 which confirms that a high degree of light intensity is lost through the optical sub-system. Hence further studies could be conducted using high power light sources.

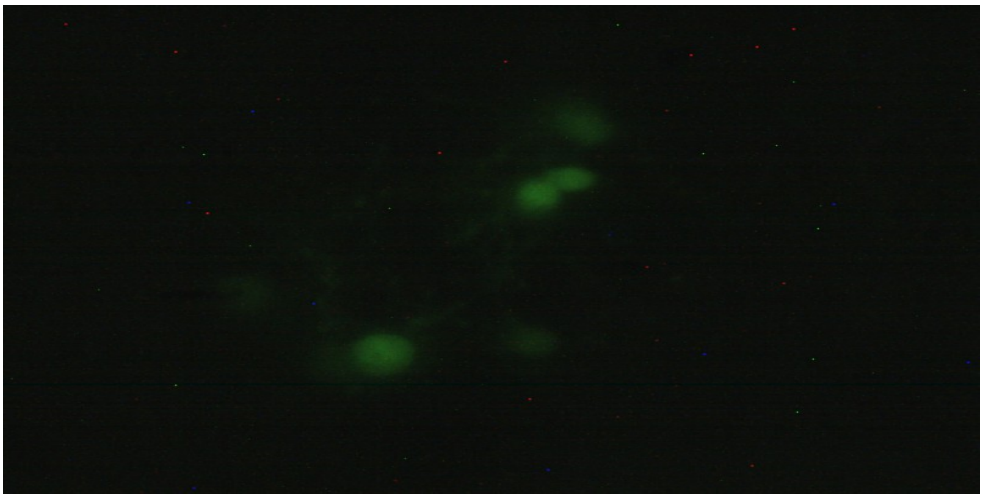

Figure 4.24 ChR2 channels expressed in primary neurons and tagged to EYFP illuminated using a strobe lamp with the fiber optic cable over the dichroic mirror (bypassing the DMD optics). The neurons were viewed under a 40X objective.

4.8 Demonstration of temporal resolution

To achieve temporal control, parts of the system were programmed using NI LabView. The parts of the system that were programmed are two strobe lamps, filter wheel and camera. The sequence in which these parts are controlled can be varied since the program is written and stored I the form of VIs. These VIs can be moved around in random orders in a flat sequence structure (NI LabView function) and the experiment conducted. In the following Graph, X-axis represents the “sequence”. The data for this Graph was obtained by adopting a particular sequence of events. The number ‘1’ on X-axis represents triggering blue wavelength strobe lamp. Similarly number ’2’ represents triggering yellow wavelength strobe lamp,’3’ represents activating the filter wheel, ‘4’ represents triggering the camera, ‘5’ represents triggering the filter wheel and ‘6’ represents triggering the camera. ‘Series 1’ to ‘Series 5’ represent the five different programmed values in milliseconds.

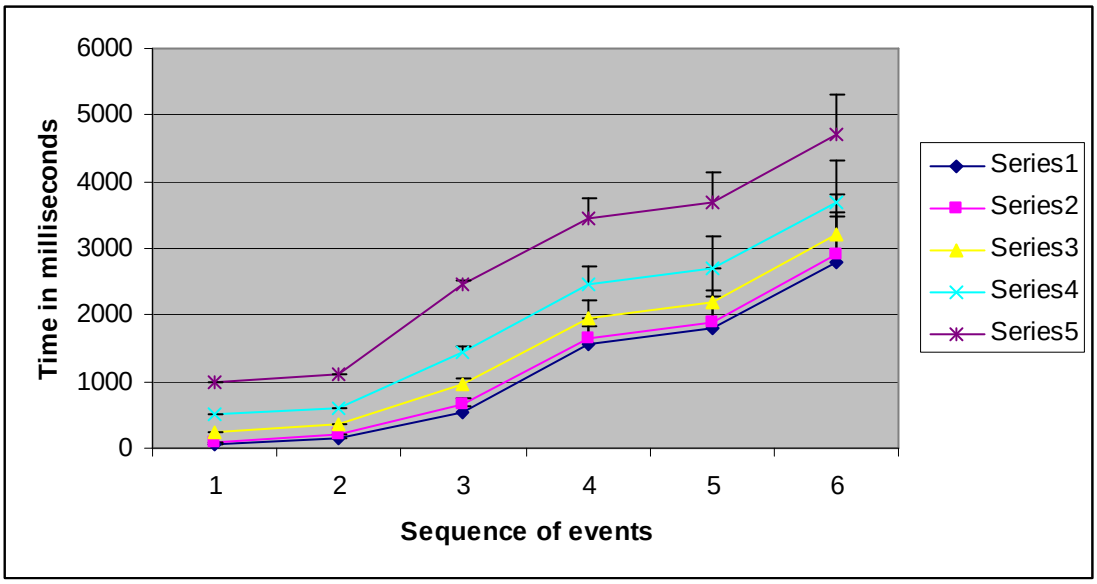

Figure 4.25 The graph depicts the temporal resolution of the system at various time points programmed in NI LabView.

The error bars represent the average error between programmed and measured error values.

Table 4.1 Represents the Sequence of events used to acquire data, the programmed values and the measured values in NI LabView.

	Series 1		**Series 2**		**Series 3**		**Series 4**		**Series 5**	
Sequences	**Pro (ms)**	**Mea (ms)**	**Pro (ms)**	**Mea (ms)**	**Pro (ms)**	**Mea (ms)**	**Pro (ms)**	**Mea (ms)**	**Pro (ms)**	**Mea (ms)**
Blue wavelength Strobe lamp	**50**	**54**	**100**	**100**	**250**	**252**	**500**	**508**	**1000**	**1000**
Yellow wavelength Strobe lamp	**150**	**152**	**200**	**204**	**350**	**360**	**600**	**606**	**1100**	**1102**
Filter wheel (340nm)	**550**	**642**	**650**	**740**	**950**	**1048**	**1450**	**1538**	**2450**	**2520**
SenSys Camera	**1550**	**1842**	**1650**	**1940**	**1950**	**2220**	**2450**	**2726**	**3450**	**3750**
Filter wheel (380nm)	**1800**	**2272**	**1900**	**2380**	**2200**	**2712**	**2700**	**3178**	**3700**	**4150**
SenSys Camera	**2800**	**3472**	**2900**	**3550**	**3200**	**3812**	**3700**	**4308**	**4700**	**5300**

The above data was obtained using NI LabView program, HPS40 oscilloscope, a photocell with voltage divider circuit to measure changes in voltage across the photocell with varying intensity of light. Thus a plot of voltage vs. time was registered on the oscilloscope and the data analyzed that resulted in Figure 4.25 and Table 4.1.

CHAPTER 5

CONCLUSIONS AND FUTURE GOALS

Nanopatterning system is a novel instrument with a unique application in Neurobiology. It could be used as an all-optical tool for high precision spatial and temporal control of neural circuitry. With its high precision spatial resolution, this system provides new avenues for controlling neural circuits with a single cell or organelle level precision. Also, the system could be used to study neuronal communication by selectively targeting single or multiple neurons.

With powerful light sources and with a UV transmittance fiber optic cable on the system, it could prove to be a potential replacement to patch clamping techniques of electrophysiology. It is worth noting that tagging ChR2 with mCherry (Promoter: NSE) and tagging NpHR with EYFP would prove useful in having a bidirectional control. Currently, researchers at UTSW successfully tagged ChR2 with EYFP and NpHR with EYFP (Promoter: NSE). However, tagging ChR2 with mCherry did not yield any red fluorescence. Another improvement that could be made on the system is working with brain slices instead of studying cultured neurons. This would help decode the natural neural network in the brain slices. These improvements on the system would render the Nanopatterning system, a powerful tool in Neurophysiology to study neurological communication and memory.

Apart from bidirectional control, Infrared Nerve Stimulation (INS) could also be studied on the system. By simply replacing the optics compatible to Infrared wavelength, the system could be turned into an Infrared Nerve Stimulating system. Ever since the researchers discovered that peripheral neurons respond to infrared light, much emphasis is being laid on studying the action mechanism of Infrared Nerve Stimulation. Thus, INS would be a topic to explore on the system.

APPENDIX A

PRODUCTS USED FOR GENETICALLY ENGINEERING NEURONS

Product Name	Concentration	Vendor/Donor
Fugene 6 Reagent	1.0ml	Roche Diagnostics GmbH
DMEM with 4500mg glucose/L,110mg sodium pyruvate/L and L-glutamine	500ml	Sigma
Trypsin EDTA,1X	100ml	Cellgro
PBS pH7.4 -calcium chloride -magnesium chloride	500ml	Invitrogen(GIBCO)
Penstrep 10000 I.U/mL penicillin 10000 ug/mL streptomycin	100ml	Cellgro
DH5-alpha	Eppendorph tubes	Kodadek lab
C34:FUGW:pUb-ChR2(H134R)-EYFP	Could be increased using DH5-alpha	Herz lab
C17:FCK(1.3)-VChR1-mCherry-W	“	“
C18: FCK(1.3)-VChR1-EYFP-W	“	“
C20:pAAV-EF1a-double floxed ChR2-mCherry-WPRE	“	“
C21: pAAV-EF1a-double floxed ChR2-EYFP-WPRE	“	“
Empty vector plasmid construct	“	“
Fetal Bovine serum	500ml	Sigma
Primer 1:ChR2+EYFP+F	-	eurofins
Primer 2:ChR2+EYFP+R	-	eurofins
ACSF	500ml	Garner lab

APPENDIX B

PROTOCOL: PLASMID DNA PURIFICATION USING THE QIAPREP SPIN MINIPREP KIT AND A MICROCENTRIFUGE

This protocol is designed for purification of up to 20 µg of high-copy plasmid DNA from 1–5 ml overnight cultures of E. coli in LB (Luria-Bertani) medium.

Note: All protocol steps should be carried out at room temperature.

Procedure:

1. Resuspend pelleted bacterial cells in 250 µl Buffer P1 and transfer to a microcentrifuge tube.

Ensure that RNase A has been added to Buffer P1. No cell clumps should be visible after resuspension of the pellet.

If LyseBlue reagent has been added to Buffer P1, vigorously shake the buffer bottle to ensure LyseBlue particles are completely dissolved. The bacteria should be resuspended completely by vortexing or pipetting up and down until no cell clumps remain.

2. Add 250 µl Buffer P2 and mix thoroughly by inverting the tube 4–6 times. Mix gently by inverting the tube. Do not vortex, as this will result in shearing of genomic DNA. If necessary, continue inverting the tube until the solution becomes viscous and slightly clear. Do not allow the lysis reaction to proceed for more than 5 min.

If LyseBlue has been added to Buffer P1 the cell suspension will turn blue after addition of Buffer P2. Mixing should result in a homogeneously colored suspension. If the suspension contains localized colorless regions or if brownish cell clumps are still visible, continue mixing the solution until a homogeneously colored suspension is achieved.

3. Add 350 µl Buffer N3 and mix immediately and thoroughly by inverting the tube 4–6 times.

To avoid localized precipitation, mix the solution thoroughly, immediately after addition of Buffer N3. Large culture volumes (e.g. ≥5 ml) may require inverting up to 10 times. The solution should become cloudy.

If LyseBlue reagent has been used, the suspension should be mixed until all trace of blue has gone and the suspension is colorless. A homogeneous colorless suspension indicates that the SDS has been effectively precipitated.

4. Centrifuge for 10 min at 13,000 rpm (~17,900 x g) in a table-top microcentrifuge. A compact white pellet will form.

5. Apply the supernatants from step 4 to the QIAprep spin column by decanting or pipetting.

6. Centrifuge for 30–60 s. Discard the flow-through.

7. Recommended: Wash the QIAprep spin column by adding 0.5 ml Buffer PB and centrifuging for 30–60 s. Discard the flow-through.

This step is necessary to remove trace nuclease activity when using endA+ strains such as the JM series, HB101 and its derivatives, or any wild-type strain, which have high levels of nuclease activity or high carbohydrate content. Host strains such as XL-1 Blue and DH5α™ do not require this additional wash step.

8. Wash QIAprep spin column by adding 0.75 ml Buffer PE and centrifuging for 30–60 s.

9. Discard the flow-through, and centrifuge for an additional 1 min to remove residual wash buffer.

Important: Residual wash buffer will not be completely removed unless the flow-through is discarded before this additional centrifugation. Residual ethanol from Buffer PE may inhibit subsequent enzymatic reactions.

10. Place the QIAprep column in a clean 1.5 ml microcentrifuge tube. To elute DNA, add 50 µl Buffer EB (10 mM Tris·Cl, pH 8.5) or water to the center of each QIAprep spin column, let stand for 1 min, and centrifuge for 1 min.

APPENDIX C

MAKING AGAR PLATES AND POURING THE PLATES

Batch makes about 40 plates.

Making the LB Agar

1. Add 250 mL of dH2O to a graduated cylinder.

2. Weigh out 20g of premix LB Agar powder (VWR DF0445-17) or:

3. 5.0 g tryptone

4. 2.5 g yeast extract

5. 5.0 g NaCl

6. 7.5 g agar

7. Mix powder well to bring into solution

8. Add dH2O to total volume of 500 mL and transfer to 1 L flask

9. Put on stirring hot plate and heat to boil for 1 min while stirring.

10. Transfer to 1 L pyrex jar and label with autoclave tape.

11. Autoclave at liquid setting for 20 minutes in a basin making sure to loosen top

12. Let agar cool to ~55C (you should be able to pick up the jar without a glove)

Pouring the Plates

1. Make sure bench top has wiped down with bleach/EtOH.

2. Remove sterile Petri dishes (VWR 25384-208) from plastic bag (save the bag for storage).

3. Pour a thin layer (5mm) of LB Agar (~10mL) into each plate being careful to not lift the cover off excessively (you should be able to just open up enough to pour).

4. Swirl plate in a circular motion to distribute agar on bottom completely.

5. Let each plate cool until its solid (~20 minutes) then flip so as to avoid condensation on the agar.

6. Store plates in plastic bags in fridge with: name, date and contents (note any additive).

Special Additives (to be added to LB Agar right before pouring plates):

- Ampicillin (VWR 80055-786) 50 mg dissolved in a small amount of dH2O (Concentration 100 ug/mL)
- X-gal (VWR IB02260) 50 mg dissolved in a small amount of DMSO Stock solutions
- Ampicillin 20mg/mL 200mg in 10mL dH2O (store at 4 in 1mL aliquots) use 50uL on each plate
- IPTG (VWR EM-5800) 100mM 238 mg IPTG in 10mL dH2O (store at –20 in 1mL aliquots) use 40uL on each plate
- X-gal 40 mg/mL 400 mg X-gal in 10mL DMSO (store at –20 in 1mL aliquots foil wrapped tubes) use 40uL on each plate

APPENDIX D

TRANSFORMATION PROTOCOL FOR DH5 ALPHA (E. COLI STRAIN)

1. Thaw bugs (E. coli) on ice.

2. Aliquot 100µl cells into pre-chilled 1.5 ml tube. Put excess bugs back into the -70 freezer.

3. Add DNA (1 to 5 µl), swirl tube, incubate on ice for 20 minutes.

4. Heat shock the cells at 42˚C for 40 seconds.

5. Add 1ml SOC; (then transfer to larger tube).

6. Rescue at 37˚C for 1 hour, shaking.

7. Spread 50µl, 100µl, (& remainder spun down if difficult ligation) on (LB+Amp) plates, --> 37˚C ON.

REFERENCES

1) Grinvald et al., Optical Imaging of Neuronal Activity. Physiological reviews,Vol.68, No.4, October 1988.
2) Sokoloff L. Relation between physiological function and energy metabolism in the central nervous system. J. Neurochem. 19: 13-26,1977
3) Lancet.D et al., Mapping of odor related neuronal activity in the olfactory bulb by high resolution 2- deoxyglucose autoradiography. Proc. Natl.Acad.Sci.USA 79:67-674, 1982
4) Sejnowski, T.J. et al., Localization of 2-deoxyglucose in single molluscan neurons. Nature Lond.287: 449-451,1980
5) Hill, D et al., Opacity changes in stimulated nerve. J.Physiol. Lond. 108: 278-281,1949
6) Tasaki et al., Changes in fluorescence turbidity and birefringence associated with nerve excitation. Proc. Natl.Acad. Sci, USA 61: 883-888,1968
7) Patrick et al., Changes in extrinsic fluorescence intensity of the electroplax membrane during electrical excitation. J.Membr. Biol 5:102-120, 1971
8) GRINVALD, A., AND I. FARBER. Optical recording of Ca^{2+} action potentials from growth cones of cultured neurons using a laser microbeam. Science Wash. DC 212:1164-1169, 1981
9) Grinvald, A, et al., Fluorescence monitoring of electrical responses from small neurons and their processes. Biophys. J. 42: 195-198, 1983.
10) Grinvald, A, et al., Real time optical mapping of neuronal activity in the mammalian visual cortex invitro and invivo. Soc. Neurosci. Abstr.11:8,1985,
11) Grinvald, A, et al.,Improved fluorescent probes for the measurement of rapid changes in membrane potential. Biophys. J.39: 301-308, 1982.

12) Grinvald, A, et al.,Functional architecture of cortex revealed by optical imaging of intrinsic signals. Nature Lond. 324: 361-364, 1986

13) Grinvald, A, et al., Simultaneous recording from several neurons in an invertebrate Central Nervous System. Nature Lond. 268: 140-142, 1977

14) London, J et al., Simultaneous optical recording of activity during feeding in Navanax. J. neurosci. 7: 649-661, 1987

15) Salzberg, B.M et al., Optical recording of neuronal activiy in an invertebrate central nervous system; simultaneous monitoring of several neurons. J. Neuro-physiol. 40: 1281-1291, 1977

16) Grinvald et al., Visualization of the spread of electrical activity in rat hippocampal slices by voltage sensitive optical probes. J. Physiol. Lond. 333:269-291, 1982

17) Salzberg,B.M et al., Optical recording of action potentials from vertebrate nerve terminals using potentiometric probes provides evidence for sodium and calcium components. Nature Lond. 306: 36-39,1983

18) Blasdel, G.G et al., Voltage-sensitive dyes reveal a modular organization in monkey striate cortex. Nature Lond. 321:579-585,1986

19) Grinvald et al., Real time optical imaging of naturally evoked electrical activity in the intact frog brain. Nature Lond. 308: 848-850,1984

20) Orbach,H et al., Simultaneous cortical monitoring of activity from many areas of the salamander olfactory bulb. A new method for studying functional organization in the vertebrate CNS.J. Neurosci.3: 2251-2262,1983

21) Orbach,H et al., Optical recording of evoked activity in the vertebral cortex of the rat (abstr.). Biol.Bull.Woods Hole 163:389,1982

22) Raichle. M et al., Quantitative in vivo autoradiography with positron emission tomography. Brain Res. Rev. 1: 47-68, 1979

23) Sawusch et al., Functional neuroimaging of attention in the auditory modality. 5 January 1998 - Volume 9 - Issue 1 - p 121-126.Auditory and Vestibular Systems, Lateral Line

24) Hemodynamic response: http://en.wikipedia.org/wiki/Hemodynamic_response

25) Functional Magnetic Resonance Imaging: http://en.wikipedia.org/wiki/Functional_magnetic_resonance_imaging

26) Cohen et al., Changes in axon fluorescence during activity; molecular probes of membrane potential. J.Membr. Biol.19:1-36,1974

27) Davila et al., Changes in ANS and TNS fluorescence in giant axons from Loligo. J.Membr. Biol.15: 29-46,1974

28) Ehrenberg et al., A microsecond kinetic study of the photogenerated membrane potential of bacteriorhodopsin with a fast responding dye. Photochem. Photobiol.39:199-205, 1984

29) Loew et al., Fluorometric analysis of transferable membrane pores. Biochemistry 24:2101-2104,1985

30) Ross, W et al., Changes in absorption, fluorescence, dichromism and birefringence in stained axons: optical measurement of membrane potential. J.Membr. Biol. 33: 141-183, 1977

31) Calcium Imaging: http://en.wikipedia.org/wiki/Calcium_imaging

32) Calcium Signaling, second edition by James W. Putney

33) Gailly et al., Critical evaluation of cytosolic calcium determination in resting muscle fibres from normal and dystrophic (mdx) mice.Cell-Calcium. 1993 Jun; 14(6): 473-83

34) Grykiewicz et al. (1985) A new generation of Ca^{2+} indicators with greatly improved fluorescence properties J. Biol. Chem, 260, 3440-3450.

35) Andersen.P et al., Lamellar organization of hippocampal excitatory pathways. Exp. Brain Res. 13:208-221, 1971.

36) Andersen.P et al., Possible mechanisms for long-lasting potentiation osf synaptic transmission in hippocampal slices from guinea-pig. J.Physiol.Lond.302: 463-482,1980

37) Dingledine et al., Brain Slices. New York: Plenum, 1984.

38) Yamamoto, C. Intracellular study of seizure-like after-discharges elicited in thin hippocampal sections in vitro. Exp. Neurol. 35: 154- 164, 1972

39) Rockland, K. S et al., Widespread periodic intrinsic connections in the tree shrew visual cortex. Science Wash. DC 215:1532-1534, 1982

40) Orbach, H , Monitoring electrical activity in rat cerebral cortex. In: Spectroscopic Membrane Probes edited by L.M.Loew. Boca Raton: CRC,1988, vol.III,p 115-136

41) R.Uma Maheswari et al, Observation of subcellular nanostructure of single neurons with an illumination mode photon scanning tunneling microscope. Optics Communications Volume 120, Issues 5-6, 1 November 1995, Pages 325-334

42) Denk et al, Photon Upmanship: Techreview Why Multiphoton Imaging Is More than a Gimmick. Neuron, Vol. 18, 351–357, March, 1997

43) Jonathan Wells et al., Pulsed laser versus electrical energy for peripheral nerve stimulation. Journal of Neuroscience Methods Volume 163, Issue 2, 30 July 2007, Pages 326-337

44) Zhang et al., Channelrhodopsin-2 and optical control of excitable cells. Nature Methods - 3, 785 - 792 (2006)

45) Mathew Banghart et al., Light-activated ion channels for remote control of neuronal firing. Nature Neuroscience **7**, 1381 - 1386 (2004)

46) Karl Deissoroth et al., Next-Generation Optical Technologies for Illuminating Genetically Targeted Brain Circuits. The Journal of Neuroscience, October 11, 2006, 26(41):10380-10386

47) Xiang Li et al., Fast noninvasive activation and inhibition of neural and network activity by vertebrate rhodopsin and green algae channelrhodopsin. PNAS December 6, 2005 vol. 102; no. 49; pages: 17816-17821

48) Konstantin Nikolic et al., Photocycles of Channelrhodopsin-2. Photochemistry and Photobiology, 2009, 85: 400–411

49) Xue Han et al., Multiple-Color Optical Activation, Silencing, and Desynchronization of Neural Activity, with Single-Spike Temporal Resolution. PLoS ONE 2(3): e299. doi:10.1371/journal.pone.0000299

50) Zhang et al., Multimodal fast optical interrogation of neural circuitry. Nature 446, 633-639 (5 April 2007) | doi:10.1038/nature05744

51) Gi/o protein: http://en.wikipedia.org/wiki/Gi_alpha_subunit

52) Ed Boyden et al., Millisecond-timescale, genetically targeted optical control of neural activity. Nature Neuroscience 8, 1263 - 1268 (2005)

53) Hodgkin AL, Huxley AF (1952) A quantitative description of membrane current and its application to conduction and excitation in nerve. J Physiol 117:500-44

54) Ernst Niggli, LOCALIZED INTRACELLULAR CALCIUM SIGNALING IN MUSCLE: Calcium Sparks and Calcium Quarks. Annual Review of Physiology Vol. 61: 311-335 (Volume publication date March 1999)

55) DMD operation manual (Texas Instruments)

56) “Sub-cellular light activation, control and manipulation using a Dynamically Reconfigurable Nanopatterning System”, a thesis by Miss Amruta Joshi (July 11, 2008)

57) “Construction and Evaluation of an Automated Light Directed Protein- Detecting Microarray Synthesizer”, a thesis by Nishanth Marthandan(July 20,2006)

58) Digital Light Processing™: A New MEMS-Based Display Technology by Larry J.Hornbeck, Texas Instruments.

59) Strobe lamp specifications:

http://www.comfilter.pl/stroboskopy/pdf/lampy_stroboskopowe_x_strobe.pdf

60) NI USB-6008 Digital control board:

http://sine.ni.com/nips/cds/view/p/lang/en/nid/14604

61) Photometrics SenSys camera manual

62) Alison Abbott, Proteins make light work of nerve control. Nature 446, 588-589 (5 April 2007)

BIOGRAPHICAL INFORMATION

NagaSandhya Mitnala, the author, has to her credit the Bachelor of Biomedical Engineering degree that she earned at Gokaraju Rangaraju Institute of Engineering and Technology (JNTU affiliated), Hyderabad, India, in August 2005. She joined The University of Texas at Arlington in the Spring 2007 semester, to pursue Masters Degree in Biomedical Engineering. Current research focus pertains to the work in the field of BioInstrumentation. Other research inclinations include Medical Imaging and Biomechanics. While in India, she introduced FEA (Finite Element Analysis) to the Biomechanics Department at MIDHANI (Mishra Dhathu Nigam Limited), a Government of India Enterprise. The introduction effectively changed the procedure for releasing Bioprosthetics by MIDHANI into the Indian Market.